AFIT/GCS/ENG/97D-11

MICRO-ELECTROMECHANICAL SWITCHES FOR MICRO-SATELLITE POWER

TRANSFER

THESIS

Presented to the Faculty of the Graduate School of Engineering

of the Air Force Institute of Technology

Air University

In Partial Fulfillment of the

Requirements for the Degree of

Master of Science in Electrical Engineering

Glen A. Kading, BS EE

Captain, USAF

December 1997

MICRO-ELECTROMECHANICAL SWITCHES
FOR MICRO-SATELLITE POWER TRANSFER

THESIS

Glen A. Kading, BS EE
Captain, USAF

19980210 048

AFIT/GCS/ENG/97D-11
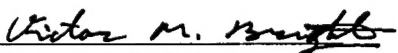
The views expressed in this thesis are those of the author and do not reflect the official

policy or position of the Department of Defense or the U. S. Government

# MICRO-ELECTROMECHANICAL SWITCHES FOR MICRO-SATELLITE

# POWER TRANSFER

Glen A. Kading B.S., M.S.
Captain, USAF

Victor M. Bright, Chairman

24 Nov. '97
date

Donald S. Gelosh, Member

24 Nov 97
date

Matthew Kabrisky, Member

24 Nov 97
date

# ACKNOWLEDGMENTS

I would like to acknowledge the efforts of my research advisor, Dr. Victor Bright, for his guidance and inspiration during the course of my research at AFIT. He kept my schedule on track with his constant attention to the details of my research and served as an excellent reviewer of all written material I have produced. Without his help I would have been doubtlessly dissatisfied with the outcome of my research.

I would also like to thank the MEMS doctoral students for their invaluable help and expertise in this field. My heartfelt thanks to Major William Cowan, Major David Burns, and Captain Jeffery Butler for all the time they have spent coaching me on the intricacies of design and testing of MEMS devices. Their corporate knowledge will indeed be sorely missed upon their graduation.

In a similar manner I would like to thank my counterparts in the VLSI group who helped me through the tough times in the lab, as they were always there to help. I would like to give a hearty thanks to the rest of the MEMS group, especially Captain Joseph Bouchard for his unending dedication and the example that this has given me in my research.

To my wife Doris, and son Duncan, I humbly thank for the understanding and tolerance they have given me during the course of my AFIT stays. They has ever been supportive of my efforts and deserve more thanks than they will ever know. I owe all of my accomplishments, both at AFIT and elsewhere to them.

# Table of Contents

# Table of Figures

# Table of Tables

# *Abstract*

In the past few years, micro-electromechanical systems (MEMS) have emerged as a promising new technology with tremendous application potential. One of the possible implementations of MEMS technology is in the development of micro-satellites. It should be possible to mass-produce micro-satellites at a fraction of the cost of one conventional satellite. In order for satellites to be robust, a method of transferring power to systems must be addressed. As micro-satellites are made with conventional integrated circuit technologies at a very small scale, a means of transferring power on a similar scale will be investigated. This research addresses the issue of the design, fabrication, and testing of a MEMS switch for space-based micro-satellites.

Devices are designed and submitted to the Microelectronics Corporation of North Carolina for fabrication. Several different design approaches are attempted, including those using electrostatic and thermal properties for actuation. Fabricated devices are tested using a microprobe station for power usage, power transfer, and frequency characteristics. Devices produce a wide range of results, the best of which transfer large amounts of power in a wide range of frequencies including DC. Recommendations are made to the sponsor agency including the most appropriate designs for use in micro-satellite applications.

# MICRO-ELECTROMECHANICAL SWITCHES FOR MICRO-SATELLITE POWER TRANSFER

## *1. Introduction*

### *1.1. Background*

In recent years, micro-electromechanical systems (MEMS) have emerged as a new technology with tremendous application potential. One of these applications is for micro-satellites (μSats). These μSats have several possible advantages over conventional satellites. First, the μSats will be several orders of magnitude smaller than the smallest satellites currently in space. Second, μSats will be mass-produced at a fraction of the cost of a single conventional satellite. Finally, several μSats can be dispersed at one time to enhance the longevity and reliability of the satellite constellation.

A problem that has been encountered in the development of these μSats is power transfer. A reliable method of transferring power with little or no losses and very low power consumption has not yet been discovered. This problem needs to be overcome for a μSat to be a viable alternative to the current macro-level satellite. Conventional methods of power transfer using integrated circuitry and macro-level switches are currently unrealistic due to excessive sizes and high currents. The limits of downscaling devices is currently in the millimeter range, with a current draw on the order of an Ampere as implemented by Hosaka and Kuwano [1]. An approach using the same

technologies as for the μSats is one avenue of implementing smaller  switches. This will keep the scale on the same order of magnitude as the μSats and keep power consumption low by electrical isolation of switches.

## 1.2.    Problem Statement

The current state of the art for satellites is on a macroscopic level.  These satellites are large and cumbersome, costing the taxpayer tens of millions of dollars in development cost, and comparable costs for launch of the device.  It is in the interest of the U. S. Air Force to design and build smaller satellites that can be mass produced at a fraction of the cost of today's conventional satellites.  These satellites will need to work in cooperation with each other to provide the coverage of a conventional satellite, and reliability must be stressed.  To this end, such μSats must have redundant systems in the event of primary system failure.  In addition, μSats will have the opportunity to be launched with other satellite systems, thus reducing the cost of launch by several orders of magnitude.

Redundant systems in the μSats must be appropriately switched off when a failure occurs in the unit and on when a redundant circuit is required to operate.  Because radiation effects, such as solar flares and other transient effects, upon these devices will be of concern, it is also likely that the failed circuits will become operational with time. Due to this probability, failed units must be available to be reactivated.

## 1.3.    Scope

This project consists of the design and fabrication of micro-electromechanical switches for the development of a space-based MEMS relay.  The design of these switches is based upon conventional switch technology adapted to MEMS scaling using the fabrication techniques available to the Air Force Institute of Technology (AFIT). These available fabrication techniques include surface micromachining using a 3-level polycrystalline silicon (polysilicon) process (MUMPs:  Multi-User MEMS Process) and a deep x-ray lithography nickel plating process (LIGA), both available through the Microelectronics Corporation of North Carolina (MCNC).  Chapter 2 includes details of these processing techniques.

There have been several attempts to fabricate microswitches and microrelays using micromachining processes.  Minimum size requirements for MUMPs die, and post-release conditions have had a significant effect on the outcome of devices, leading to high actuation voltages and improper operation [2].  The ideas behind these applications have been studied and improved upon in this thesis, where applicable, to create MEMS relays that are acceptable for use in a μSat application.  Special attention is placed upon actuation voltages and currents, signal carrying capability, and contact resistance in each structure.

## 1.4.    Assumptions

Due to the nature of this research, several assumptions concerning the electrical and mechanical properties of materials in the fabrication process were made.  The MCNC

sponsored process has varying process factors that determine characteristics such as resistivity and Young's modulus [3]. It must be assumed these factors have little variance between runs and die in the same facility. Thus, electrical parameters investigated in previous work for actuation potential of thermal actuators are assumed to be unchanged.

Some structures will be plated with a thin layer of nickel using the Nickelex ™ electroless plating solution. Although addition of a nickel plating will increase current drain of thermal actuators and reduce contact resistance, it is assumed that the thermal actuators will operate on the same principle as an unplated polysilicon actuator--thus no new modeling of thermal actuators is necessary.

### 1.5.    Approach

The devices created to achieve a switching action on a MUMPs die include a flip-wire switch, rotary switch, simple latching switch, gripping switch, bridge actuator, and fork switch. These devices were chosen for their ability to provide a large amount of contact area, their impedance characteristics, and their ease of fabrication.

The basic principle of all designs is to bring the largest area of two contacts together, preferably with a low resistance contact, while minimizing necessary actuation forces. The amount of contact area has a direct effect on contact resistance, and actuation force is limited by structure geometry and fabrication content. It is necessary that little or no power be required to hold switches open or closed to allow both AC and DC operation with no interference.

CADENCE, a design suite that allows use of circles and curves, was used in the design of these structures. Many variations of each design were tested to ensure maximum coverage of design parameters and to help determine the optimum performance range for each device. This design tool can be used for both LIGA and MUMPs designs, but MCNC was not able to provide an acceptable LIGA run. Therefore, three MUMPs and no LIGA runs were used in this research.

Tests performed include measuring electrical resistance and capacitance, and determining the frequency range of each device. Proper operation of each device is also tested. Once the devices are characterized, revisions are made to designs to improve operation and correct defects. Finally, recommendations are made for those devices that will be most appropriate for use in the transfer of power for μSats.

## 2.Literature Review of Technologies Applicable to Microrelay Development

Switches and relays have been in use on a macroscopic scale since the discovery of electricity to switch currents on and off in an electrical circuit. The earliest power switches were simple hinged or cantilever beams, arranged to close an open circuit [4]. These primitive power switches later evolved into blade-and-jaw switches that are still common in high power applications today, shown in Figure 2.1.
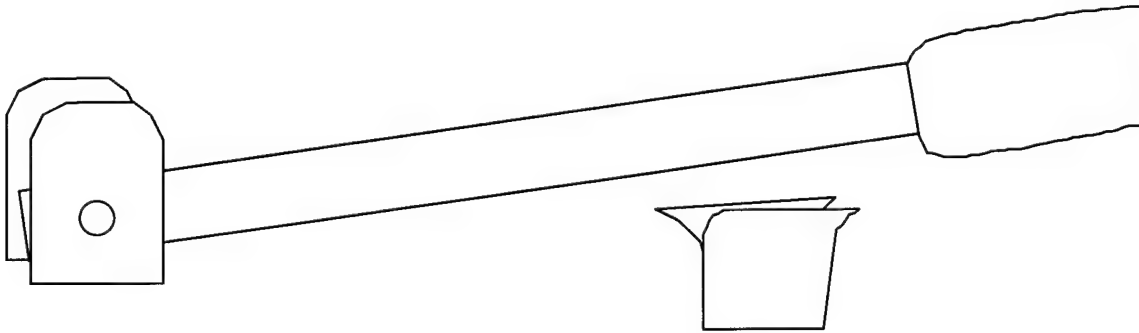
**Figure 2.1:** Blade-and-jaw switch.

Most electrical and electronic circuits today use an evolved form of this switch called a micro-switch or micro-relay. This switch normally has components consisting of contacts, springs, and some sort of bridging device. The terminology used to classify switches can be understood through Figure 2.2 and the following definitions. Pole denotes the number of completely separate circuits that can pass through the switch at the same time. Throw denotes the number of different circuits that each individual pole can control. Break denotes the number of pairs of separated contacts the switch introduces

into each circuit it opens [4]. The simplest relays consist of single pole, single throw, single break switches while more complex relays will have an increasing number of poles and throws. For instance, a rotary relay will have several throws while still being a single pole, single break circuit.

Most of the simple applications of switches and relays will use a single throw switch. Single and double pole switches can be used depending on the application. Double pole switches will allow more electrical isolation when the circuit is not actuated, and thus

**SINGLE-POLE**
**SINGLE-THROW**
**SINGLE-BREAK**

**DOUBLE-POLE**
**SINGLE-THROW**
**SINGLE-BREAK**

**SINGLE-POLE**
**SINGLE-THROW**
**DOUBLE-BREAK**

**DOUBLE-POLE**
**SINGLE-THROW**
**DOUBLE-BREAK**

**SINGLE-POLE**
**DOUBLE-THROW**
**SINGLE-BREAK**

**DOUBLE-POLE**
**DOUBLE-THROW**
**SINGLE-BREAK**

**SINGLE-POLE**
**DOUBLE-THROW**
**DOUBLE-BREAK**

**DOUBLE-POLE**
**DOUBLE-THROW**
**DOUBLE-BREAK**
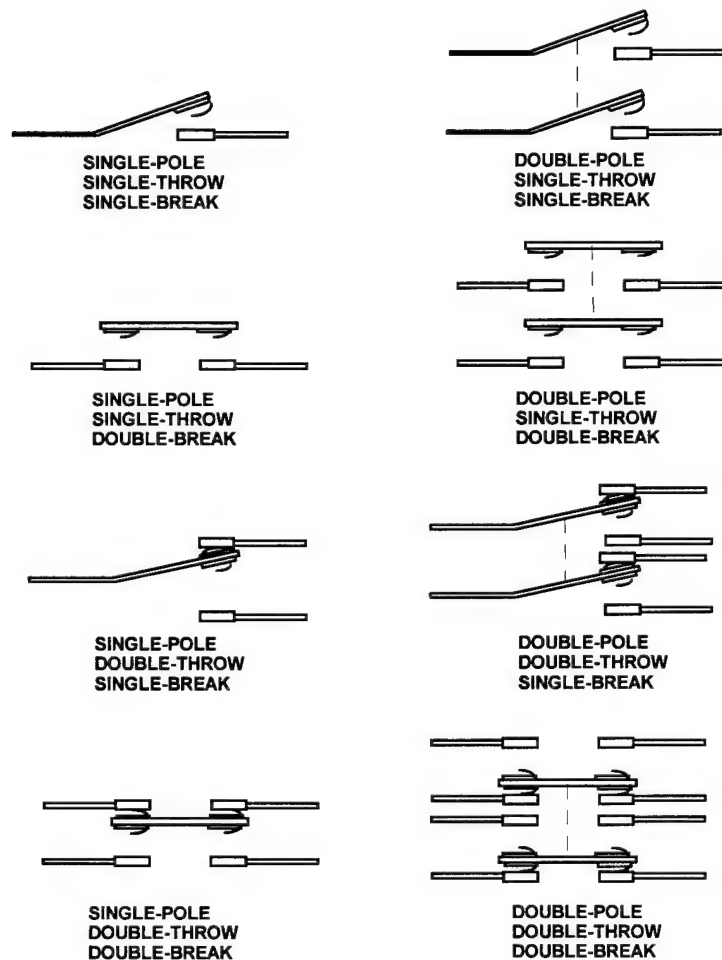
**Figure 2.2:** Poles, throws, and breaks [4].

2-2

would be more appropriate for higher voltage applications. Since it is unlikely that microscopic relays will have high voltage potentials across them, the most appropriate switches to be designed using micromachining technology are single pole and single throw. The basic principles behind these macroscopic relays can be applied to microscopic applications such as creating relays on a MEMS die. Several forms of microscopic relays have emerged in the scientific community to switch signals. For example, a matrix relay has been developed by using microsystem design and conventional machining technology [1]. This device actuates an array of switches using electromagnetic forces. Figure 2.3(a) shows the design, while Figure 2.3(b) shows the actual implementation of this device. The microrelay has advantages over conventional relays in being smaller and consuming less power [5].



(a)                          (b)
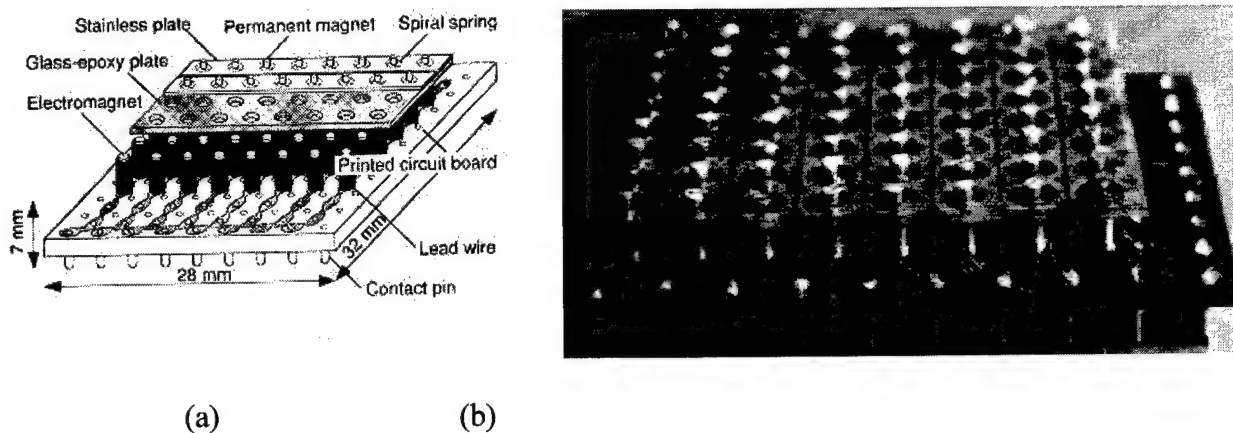
**Figure 2.3**: Electromagnetic relay using conventional machining methods [1].

Hosaka and Kuwano proposed using microelectromechanical system (MEMS) technology to fabricate mechanical relays [1]. Since a MEMS is small and its fabrication process is

special, it is suitable for integration and excellent for high-speed movement. They feel that, as a result, MEMS relays cannot generate high power or be made with complicated structures. On the other hand, signal processing relays handle information and thus do not require high output power [1]. High output power is a relative term, and a μSat will have a need for significant power for their size, but they will not need high power. These satellites should be working with low voltages and low currents, which can easily be passed by structures formed in a micromachining environment.

These relay die can be subsequently assembled as a multi-chip module (MCM) allowing it to be integrated with CMOS electronics, or fabricated with the MEMS structures that they are intended to control. This MCM process will allow use of microrelays in various applications from MEMS devices to CMOS circuitry. An approach using integrated technology (that is only currently available in custom processes) was suggested in 1993. This approach was proposed as a practical application of MEMS technology [6] by Hosaka, Kuwano, and Yanagisawa. Their design included using transistors, diodes, and microrelays on the same die. A conceptual representation of this technology is shown in Figure 2.4.
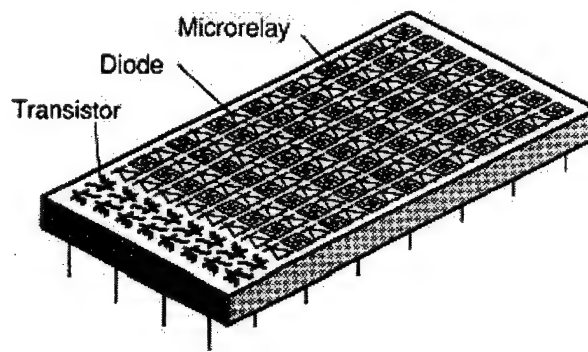


**Figure 2.4**: Possible layout of an integrated 8x8 matrix switch [6]

The MUMPs technology has a limit to the height of a moveable object, to include such features as dimple, polysilicon level 1, polysilicon level 2, and a layer of oxide trapped between these two levels of polysilicon. This maximum height for structures is thus 4.75 μm. Specifications for each layer can be seen in Table 2.1. Electrostatic actuators have a limit to the amount of force that can be attained. For devices that use electrostatic attraction between sidewalls for the driving force, increased thickness allows a greater electrostatic drive for a given bias voltage [7].

**Table 2.1**: MUMPs Thicknesses [3].

| Material Layer | Thickness (μm) | Lithography Level Name |
|---|---|---|
| Nitride | 0.6 | - |
| Poly 0 | 0.5 | POLY0(HOLE0) |
| First Oxide | 2 | DIMPLE ANCHOR1 |
| Poly 1 | 2 | POLY1(HOLE1) |
| Second Oxide | 0.75 | POLY1_POLY2_VIA ANCHOR2 |
| Poly 2 | 1.5 | POLY2(HOLE2) |
| Metal | 0.5 | METAL(HOLEM) |

Attempts have been made to miniaturize relays for use in microscopic applications for some time. Attempts include those of Hosaka and Kuwano, who decided that MEMS was not practical for their application [1]. Another group has fabricated electrostatic polysilicon microrelays integrated with MOSFETs in a custom process [8]. Gretillat, Thiebaud, Rooij, and Linder, from Switzerland, successfully integrated the two technologies. The circuit, however, is only able to pass 0.5 mA [8], which is not

sufficient for power transfer applications. Zavracky et. al. fabricated a micromechanical relay using another custom process using nickel for contacts, and a sacrificial layer of copper. This design provides relatively low current, up to 10 mA under normal atmospheric conditions [5].

A unique implementation of micromachined relays has been presented by researchers from UCLA. The system uses a mercury drop to make a mercury-contact micromechanical relay [9]. The system uses nickel heaters, in conjunction with
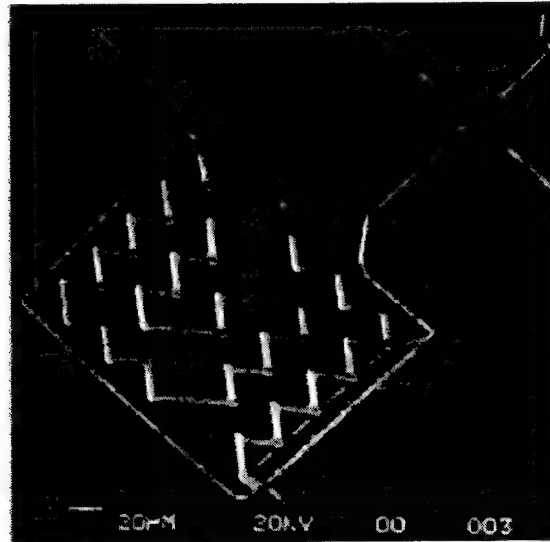


**Figure 2.5:** Micromechanical relay with thermally driven mercury micro-drop [9]

micromachined v-grooves to make a thermometer-like structure as shown in Figure 2.5. Electrodes in the center of the unit are normally in contact via the mercury drop. When current is applied to the nickel heater, a bubble will form, forcing the mercury away from the contacts. This switch allows for an on resistance of $1\Omega$, while the actuation energy dissipated is ~100 mW [9].

The premier application of microactuators lies in miniature valves, but other potential applications include miniature connectors, switches, and end effectors for microrobotic manipulators [10]. In order to develop devices that will be effective as power relays, switches and relays in general must be understood. Current switch and relay designs, from the standard single-throw light switch on the wall to high power relays in aircraft, will be studied. In application of μSats, we are interested in the transfer of DC and AC signals with a minimum amount of electrical resistance as well as a minimum average power consumption for switching. These switches must have the potential to be manufactured with current commercial processes, making them economically viable. This can be accomplished by building an electrically isolated MEMS circuitry that will actuate, driving contacts together to produce an electrical connection.

In order to achieve this goal, the MCNC MUMPs process was used. MUMPs, on the other hand, provides a more robust process and has a much better defined range of design criteria associated with it. Additionally, MUMPs libraries are available that make creating structures easier and less prone to design errors, as these libraries are already tried and true.

### 3. Theory of Device Actuation

Each design, with the exception of the flip-wire switch, employs deflection of a cantilever or beam in operation. Hence, the force necessary to move these beams must be investigated. The majority of these devices also use thermal actuation, while others use electrostatic actuation. The actuation potentials and energies must be investigated to prove that operation will occur properly.

### 3.1. Theory of Beam Deflection

A device that moves suspended material fixed at one or two ends involves the theory of beam deflection. These devices may push a cantilever beam or use the deflection in the acutation of the device itself. A cantilever beam can be simply modeled using formulas for the flexure of straight beams ignoring terms for stress.

#### 3.1.1. Theory of Cantilever Deflection

A beam of material that is solidly anchored to the substrate at one end while being unattached at the other end follows the laws of a cantilever beam. A deflection at the unanchored end of the cantilever beam can be calculated by using the force applied and properties of the subject material.

##### 3.1.1.1. Theory of End Load Deflection

As a force, F, acts on a cantilever tip, the deflection, d, can determined by the following equations [11]:

$$d = \frac{F \cdot L^3}{3 \cdot E \cdot I} \tag{3.1}$$

$$I = \frac{1}{3} \cdot w \cdot h^3 \tag{3.2}$$

where L is the length, w is the width, and h is the thickness of the cantilever, with E being the modulus of elasticity for the beam. The cross-sectional spring constant, which is a constant relation between force and deflection can be determined by substituting equation (3.2) into equation (3.1) and solving for d/F. This substitution yields the cross-sectional spring constant:

$$k_{cs} = \frac{E \cdot w \cdot h^3}{L^3} \tag{3.3}$$

This equation shows a general spring constant for a fixed cantilever with an end load, which is a function of temperature when the flexure is being heated as in vertical and horizontal thermal actuators.

### 3.1.1.2. Theory of Distributed Load Deflection

If a force, F, is distributed along the length of a cantilever, the effect is somewhat different from that of an end loaded beam. The maximum deflection can be defined as [11]:

$$d = \frac{F \cdot L^3}{8 \cdot E \cdot I} \tag{3.4}$$

This formula is essential in modeling the force necessary for electrostatic switch travel to reach a contact.

### 3.1.2. Theory of Rigid Beam Deflection.

A rigid beam is a flexure that is attached to a solid structure at both ends. A force, F, that is placed in the center of this beam induces stress similar to that of a cantilever beam. This beam has a maximum deflection of [11]:

$$d = \frac{F \cdot L^3}{192 \cdot E \cdot I} \qquad (3.5)$$

which allows us to again determine the spring constant as:

$$k = k_{cs} = \frac{192 \cdot E \cdot w \cdot t^3}{3 \cdot L^3} \qquad (3.6)$$

The equation above shows that a rigid beam has a much higher spring constant than that of a cantilever beam, and is thus much harder to move.

### 3.2. Theory of Electrostatic Actuation

Many devices made using the MEMS processes use electrostatic forces as a principle of actuation. In order to understand the operation of these devices, electrostatic forces must be computed. To simplify the solution somewhat, we can express the potential energy, $\xi$, of the charge distribution as a function of electrode voltage and charge distribution upon the plates of the actuator [12]. Thus, the potential energy can be expressed as [12]:

$$\xi = \frac{1}{2} \int_v \sigma V \, dA = \frac{1}{2} \int_v \varepsilon_0 E^2 \, dv \qquad (3.7)$$

where $\sigma$ is the surface charge distribution on the electrode plate, V is the actuation voltage between the address electrode and the electrode plate, A is the surface area of the

electrode plate, $\varepsilon_0$ is the permittivity of free space, and E is the electric field intensity at any point in the volume $v$ within the device.

Now that we have a basic equation for the energy of a device in terms of an electric field, we can use the Virtual Work [13] method to analyze the force on the surface of the electrodes. First, consider a parallel plate capacitor with a separation $x$, connected to a power source such as a battery that is supplying a fixed potential voltage V. If an external mechanical force displaces one plate by $dx$, conservation of energy states that the net energy supplied in the displacement is equal to that of the change in the stored energy of the capacitor. More precisely, this change of energy, $\xi_C$ is equal to the sum of the mechanical force applied, $\xi_F$, and the change in the energy supplied by the battery, $\xi_B$ as shown below:

$$\xi_F + \xi_B = \xi_C \tag{3.8}$$

The change in energy supplied by the battery and mechanical work relate to:

$$\xi_F = Fdx, \qquad \xi_B = VdQ \tag{3.9}$$

where the change in electric charge of the battery is defined as dQ, and is equal to the product of the applied potential voltage, V, and the change in capacitance, dC. The electrical energy of the battery, substituting in these terms can now be defined as:

$$\xi_B = V(VdC) = V^2 d\left(\frac{\varepsilon_0 A}{x}\right) = -V^2 \varepsilon_0 A \frac{dx}{x^2} = -\left(\varepsilon_0 E^2\right)(Adx) \tag{3.10}$$

Under a uniform electrical field, eq. (3.7) can be integrated to form the differential change in electrical energy as shown by:

$$\xi_C = \varepsilon_0 \frac{AV^2}{2} \left( \frac{-dx}{x^2} \right) = -\frac{\varepsilon_0 E^2}{2} A dx \tag{3.11}$$

Substituting eqs. (3.10) and (3.11) into eq. (3.8) yields

$$Fdx - \varepsilon_0 E^2 A dx = \frac{-\varepsilon_0 E^2}{2} A dx \tag{3.12}$$

Which simplifies to:

$$Fdx = \frac{\varepsilon_0 E^2}{2} A dx \tag{3.13}$$

Eq. (3.7) represents the total force on the surface of the conductors as a function of the electric field. It further demonstrates that the force per unit area on the surface of the plate is equal to the electrical energy density per unit volume within the plates [13].

### 3.3. Theory of Thermal Actuation

Micromachined devices also operate upon the principle of thermal expansion. When a material is heated, it expands, with heat being the major byproduct of resistive losses in the medium. When there is no way to easily dissipate this heat, the molecules in the material become excited, and the piece of material begins to expand. Smaller masses have more pronounced movement due to this effect. If a circuit made of a homogeneous material consists of a thin and a thick portion, conservation of current states that the same amount of current will flow through both portions of the circuit. The thin portion of the circuit will then have a higher current density which will excite molecules faster, causing the material to expand. This principal is used in the thermal actuation of devices.

Consider the thermal actuator shown in Figure 3.1. Note that the hot arm and cold arm conform to the principle described above, and thus react as indicated when current
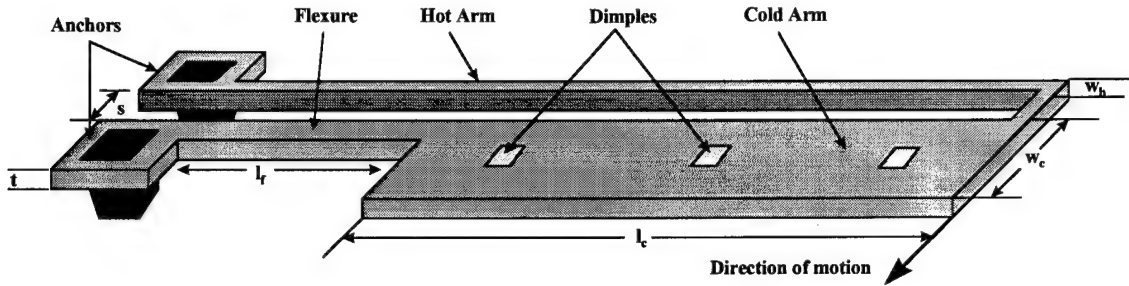


**Figure 3.1:** Horizontal heat-drive actuator [15].

is applied. By applying a constant current through the circuit of this device, it is then possible to heat the hot arm and flexure hotter than the cold arm.

An estimate for the deflection of the tip of a horizontal heat drive actuator constructed with materials of same or similar Young's modulus can be defined as [16]:

$$\delta_{Lateral} \approx \frac{3L^2(T_{HOT} - T_{COLD})\left[\lambda(T_{HOT}) - \lambda(T_{COLD})\right]}{4W_{H+F}} \tag{3.14}$$

where $T_{HOT}$ is the average temperature of the hot arm and $T_{COLD}$ is the average temperature of the cold arm and flexure. L is the length of the hot arm, and $W_{H+F}$ is the sum of the widths of the hot arm and flexure. The $\lambda$'s represent the coefficients of thermal expansion as a function of temperature [16]:

$$\lambda(T) = \left(3.725\left\{1 - e^{[-5.88x10^{-3}(T-124)]}\right\} + 5.548 \times 10^{-4} T\right) \times 10^{-6} \; (K^{-1}) \tag{3.15}$$

$T_{HOT}$ and $T_{COLD}$ can be derived from the current through the device using SPICE models developed at the Air Force Institute of Technology by Captain Jeffery Butler [16].

### 3.4. Theory of Rotary Compression Switch Actuation

The rotary compression switch is a device that uses a rotor as a method of force translation. The system can be simplified using classical physics and Newton's third law, which states "if two bodies interact, the force exerted by body 1 on body 2 is equal to and opposite the force exerted on body 1 by body 2" [17]. This law, in combination with geometry, can resolve the forces acting on this structure. Consider the system shown in Figure 3.2 below:
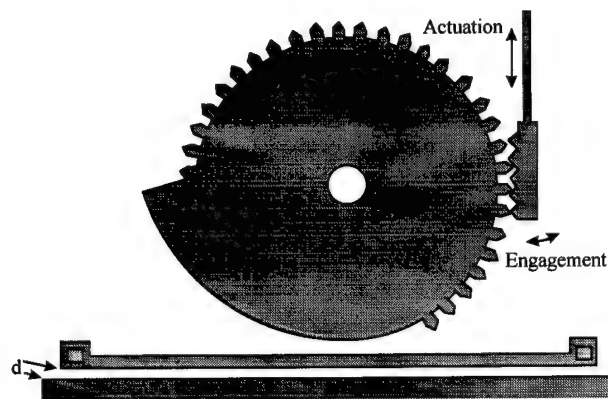
**Figure 3.2:** Rotary compression switch.

When this device turns around the axis, it puts force on the beam beneath it. We can break this down into a simple force system as shown in Figure 3.3.

F beam

F Applied

θ
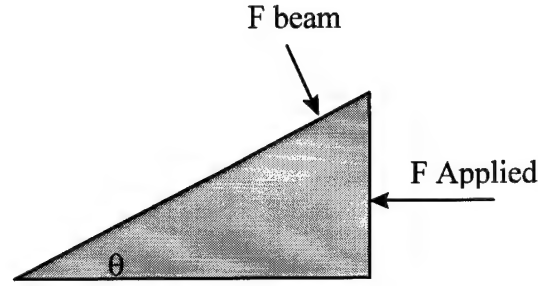
**Figure 3.3:** Simplified force system.

Using the maximum deflection Equation (3.8) for rigid beams and the angle of incidence, θ, we can determine the force necessary to move the beam to maximum deflection (d in Figure 3.2 above). If we split the normal force of the beam into components, we can see that the following relation holds:

$$F_{applied} = F_{beam} / \sin(\theta) \qquad (3.16)$$

Substituting Equation (3.8) into Equation (3.23) yields the total force necessary to move the rigid beam to maximum deflection (contacts closed).

$$F_{applied} = \frac{d \cdot 192 \cdot E \cdot I}{L^3} \Big/ \sin(\theta) \qquad (3.17)$$

Where E is the modulus of elasticity, I is defined in Equation (3.2), and L is the length of the beam.

### 3.5. *Chapter Summary*

In this chapter, the basic theory was described for calculating the electrostatic forces upon a device by modeling the capacitances of these devices. This method can be directly applied to all electrostatic devices generated during this thesis. Beam theory was also investigated, showing the forces required to move beams suspended by three

different methods. The results were then translated into the force necessary to rotate the rotary compression switch.

Chapter 4 details the steps necessary to design devices used in this research and also describes the post-processing steps required to ensure proper operation of fabricated devices. All equipment used in testing devices is detailed, as well as testing procedures used on each type of device. Finally, descriptions are provided for each device used in this research.

## 4. Experimental Setup, Procedure, and Fabrication

This chapter deals with the MEMS design process with attention to the design submission process. Processing and post-processing procedures, descriptions of the devices, testing methods, and test equipment used in the characterization of the microrelays fabricated using the MUMPs process are discussed. This chapter gives information concerning devices fabricated, their intended operational characteristics, and the methods that were used to test each device.

### 4.1. Design Process

The MUMPs submission process is similar to the processes used to submit a design to a commercial foundry. Each mask layer must be laid out and must then be digitized into a format acceptable to the fabrication facility in question. There are several Computer Aided Design (CAD) tools available to users to aid in this process. The MAGIC and CADENCE layout editors, which were originally designed for use in integrated circuit fabrication, are two tools available at AFIT. These tools allow the layout of several layers of materials displayed in the form of colored or patterned polygons. These polygons, representing distinct layers in the micromachining process, can be translated into a standardized file format. The designs submitted to MCNC are sent in the Caltech Intermediate File (CIF) format. This file, used by the foundry to create masks, can be

sent via electronic mail or File Transfer Protocol (FTP) to the fabrication facility. AFIT sends designs to MCNC through FTP.

MAGIC and CADENCE are design layout editors that were originally designed for the complimentary metal-oxide semiconductor (CMOS) fabrication process. MAGIC is an older tool that allows only manhattan geometries, limiting the user to use only right angled shapes composed of pixel like squares, while CADENCE allows the user to create different shapes such as arcs, circles, and diagonal lines. Customized technology files can be used to transform these CMOS layout editors into MEMS layout editors for the LIGA and MUMPs processes.

The MUMPs process available through MCNC allows for three layers of polysilicon
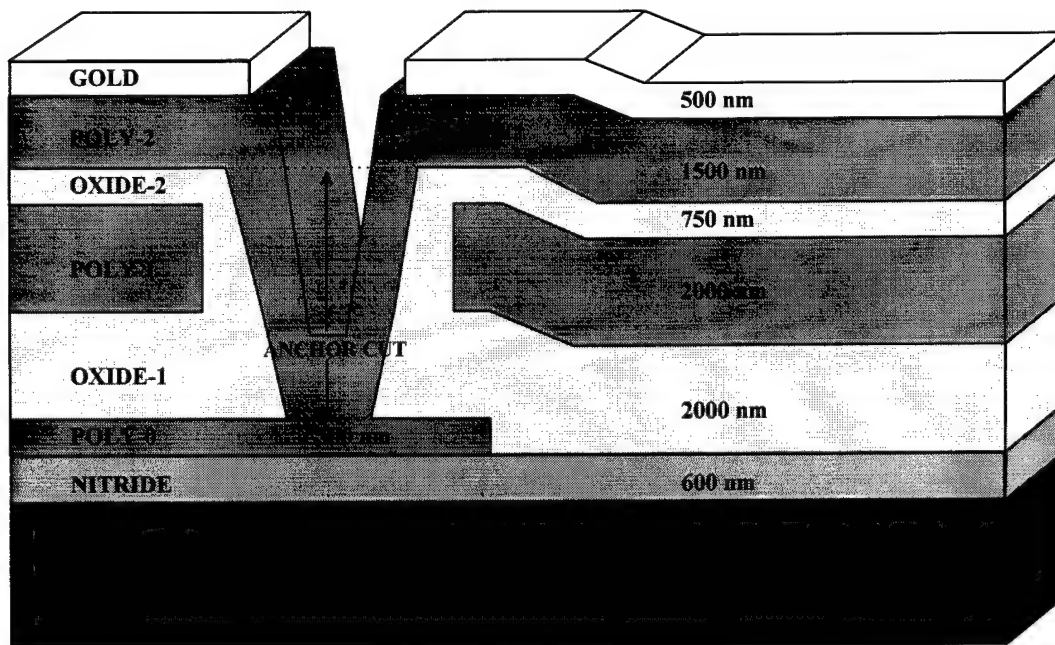


**Figure 4.1:** Cross-section of MUMPs layers including mean thickness.

and one layer of metal. Gold, used as the metal layer, is the most conductive component of the process and is only allowed to be anchored to the poly-2. The metal is the last deposited layer since it is non-refractory and the polysilicon layers are annealed at 1100°C to reduce stress [3]. Figure 4.1 shows the layer thicknesses and the major etching steps in the MUMPs process. The anchor-1 and anchor-2 cuts may be made either directly to the nitride or attached to the poly-0 layer.

## 4.2. Design Considerations

An important consideration in the design process is the placement of etch holes in large plates. The MUMPs design rules state that etch holes must be placed at a maximum of 30 μm apart [3]. From the collective experience of those testing devices at AFIT, that margin can be easily pushed to 50 μm without deleterious effects. If etch holes are not present, or are too far apart, the etchant could fail to remove all of the oxide from the die. This would leave structures fixed that were originally designed to move. Compensating for extra oxide by etching for a longer period of time could cause small silicon structures such as hinges to become too weak to support the devices intended. The devices designed have sufficiently small area to insure that etch holes will not be necessary, and are designed for a minimal release etching time.

Another consideration that is of utmost importance is the topology of layers defined in the MUMPs process. Each layer of material, including polysilicon and oxide, is deposited over existing layers, causing each successive layer to conform to the layer

underneath it. Figure 4.2 shows a sample of the typical conformity seen in the patterned

layers of polysilicon.
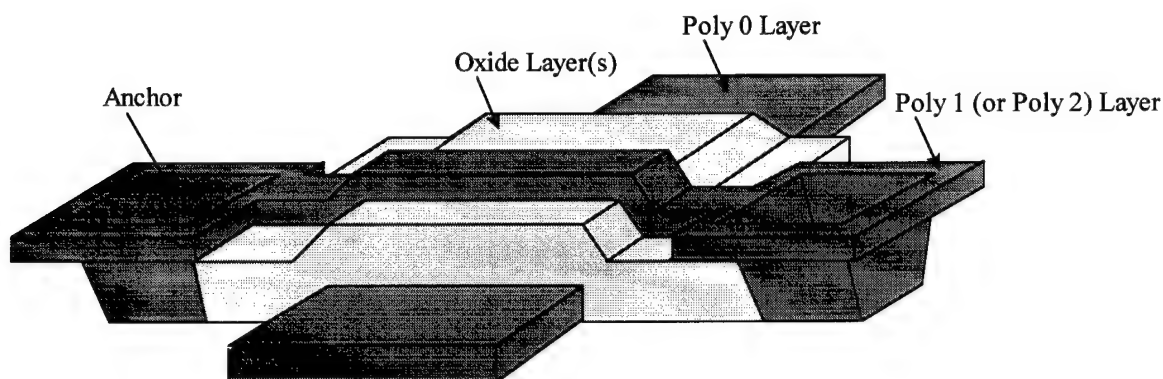


**Figure 4.2:** Conformity of polysilicon layers.

The topology of these layers can at times have adverse effects upon the creation of

devices. A mirror created to reflect a laser beam could have an uneven surface that would

scatter the beam while reflecting it normal to the mirror surface. This topology can also

have advantages when designing certain structures. For example, one can lay down a

strip of poly-1 with a poly-2 strap (replace the poly-0 in Figure 4.2 with poly-1) creating a

hinge structure.

The design rules given in the SmartMUMPs handbook [3] must be given careful

consideration in addition to the items mentioned above. The majority of these design

rules reflect the capabilities and limitations of the photolithography techniques available

to MCNC. For example, the Poly 1 layers must be at least 2 $\mu$m across and have a

spacing of 2 $\mu$m. Other limitations are caused by the tolerance in the mask alignment

process [3].

## 4.3.  Post Processing Procedures

In order for a MEMS die to operate properly, it is necessary to perform some post-processing steps.  MCNC ships the die with oxides still between the layers of polysilicon, as well as with a thick protective layer of photoresist that is intended to protect the die during shipping.  To release the structures, it is necessary to first remove the photoresist, and then etch the sacrificial silicon dioxide layers.  The release procedure can be found in Table 4.1.

**Table 4.1:** MUMPs Post Processing Steps.

| Step # | Time | Action/Compound | Amount/Temp |
|--------|------|-----------------|-------------|
| 1 | 5 minutes | First Acetone | 50 ml |
| 2 | 10 minutes | Second Acetone | 50 ml |
| 3 | 10 minutes | First Methanol | 50 ml |
| 4 | 2 minutes | Hotplate | 51° C |
| 5 | 2-5 minutes | Hydrofluoric Acid | 50 ml |
| 6 | 5 seconds | Deionized Water | > 1 litre |
| 7 | 10 minutes | Second Methanol | 50 ml |
| 8 | 2 minutes | Hotplate | 51° C |

The first step in the procedure is to remove the layer of photoresist that is protecting the die.  A fifteen minute bath in acetone ($CH_3COCH_3$) sufficiently removes the layer of photoresist.  This step is succeeded by a ten minute bath in methanol ($CH_3OH$) which can be dried on a hotplate at 51° C for two minutes (in a clean specimen dish).

Next, the release of the sacrificial $SiO_2$ is performed.  This is performed by hydrofluoric acid (49% by weight).  The die is placed in the acid for 2 to 5 minutes, depending on the size of released structures, then immediately dipped into a large vat of

water and moved to a second methanol bath for ten minutes. This step displaces water which has a very high surface tension and has a tendency to cause structures to stick to the substrate when drying. After the methanol bath, the die is placed back on the hotplate for two minutes. The die is now ready to test.

## 4.4. Experimental Setup

After devices have been fabricated and released, they must be examined, tested, and characterized. The AFIT MEMS laboratory has the necessary equipment to test these devices in a designated area. The experimental setup, as shown in Figure 4.3, was used in testing all of the devices designed during the course of this thesis. This setup utilizes the
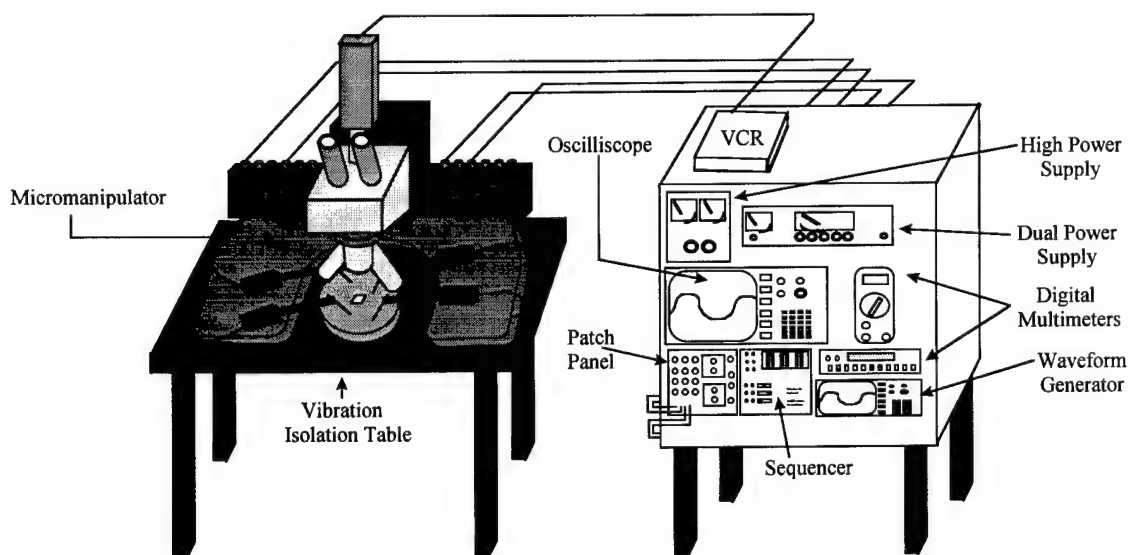


**Figure 4.3:** Experimental setup for device testing.

capabilities of the micromanipulator probe station (The Micromanipulator–Model #6200) to apply voltages to each device. This device consists of a flat platform for holding die and wafer sized objects under a vacuum, with a second platform for resting probes. The

micromanipulator has the capability of using eight different probes simultaneously, however practicality limits use to four due to crowding on the platform. Each probe consists of a vacuum mounted chuck that holds a fine needle electrically connected to a line in the station. The diameters of the needle tips range from 15 to 20 $\mu$m, which is adequate to place on a small probe pad, or on device wiring. Measurement devices and power supplies can be routed through these probes to create electrical connections and/or measure electrical characteristics.

Two different types of power supplies were used to actuate and test fabricated devices. First, a dual power supply (Hewlett Packard – Model HP 6236B) was used. This supply is essentially a combination of two different supplies. One part supplies up to +/- 6 volts and 0.5 amps, while the other supplies up to +/- 20 volts at 2.5 amps. Two of these supplies can be chained together to supply +/- 40 volts at 2.5 amps. The second supply used was a high voltage source (Kikusui Electronics Corporation – Model PAD 160-1L) that offers the option of being current or voltage limited. This supply is very useful in preventing destruction of high potential electrostatic devices. The high voltage source can supply up to ~165 volts at 1 amp.

Sequencing devices to provide mechanical power to the linear switch and rotary compression switch was necessary. A mechanical relay system controlled by 555 timers provides a means to easily generate variable duty cycle square waves. This sequencer, built by a former AFIT doctoral student [18], can be used in the normally open or normally closed mode, allowing for easy switching between modes (which allows reversal of the motors). Three channels are provided in this sequencer.

To measure the impedance characteristics of each device, it was necessary to use two digital multimeters available in the testing area. These measuring tools (Hewlett Packard – Model 3478A and Fluke – Model 8600A) were used to determine open and closed resistances of each device, actuation voltages and currents, and the voltage and current capacity of each relay. To determine frequency characteristics, the half power point was used. An input signal, supplied by a function generator (Hewlett Packard – Model 54100A) capable of supplying square, sinusoidal, and triangular waveforms at up to 20 MHz was detected using a digital oscilliscope (Hewlett Packard Model 54100A). Signals up to 10 volts peak-to-peak with a bias of up to 10 volts can be measured with this device.

Testing of an entire relay system requires bonding to a chip carrier. This is accomplished by utilizing a ball bonder (Kulicke and Soffa Industries) that uses heat, pressure, and ultrasound to bond a 25 μm thick gold wire from a MEMS die to a chip carrier package.

Finally, after devices have been tested, it is necessary to closely examine and analyze them. A scanning electron microscope (International Scientific Instruments Model WB-6) is useful for this purpose. This device allows three-dimensional viewing of released structures. To prevent charging of released structures which causes bright streaks in SEM micrographs, a 300 Å layer of gold must be sputtered. This layer effectively grounds all devices to a common plane and effectively eliminates charging problems on all but the tallest released structures.

## 4.5.    Testing Procedures

Two types of switches were investigated during the course of this research:   switches that require constant potential to maintain a contact or maintain a broken contact, and switches that can be locked in the open or closed positions.  The first type of switch can be termed "constant", meaning constant effort is necessary to actuate, while the second can be termed "locking".  A list of those devices belonging to each category can be found in Table 4.2.  "Locking" switches can pass both AC and DC sources, while "constant" switches can only operate with an AC signal source.  With all equipment, it is imperative

**Table 4.2:** Switch Classifications.

| "Constant" Switches | "Locking" Switches |
|---|---|
| Thermal Bridge Switch | Linear Flip-Switch |
| Electrostatic Flip-Switch | Rotary Compression Switch |
| Electrostatic Resist Switch | Ramp Switch |
|  | Gripper Switch |

that the operator remembers to reduce the voltages to an acceptably low level to ensure that devices do not vaporize when supplies are powered.

Some of the "constant" switches described in Section 3 operate using electrostatic potentials, while others are actuated using thermal heatuators.  Although the driving force is different in these two types of switches, the guiding principle behind them remains the same, and as such they can be tested in virtually the same manner.  The following is a list of steps that are followed when testing "constant" devices.

1. Ensure that all equipment is turned 'off' and that settings are at their minimum levels.

2. Place the die in the center of the micromanipulator table, turn on the vacuum, nitrogen, and power to the table.

3. Place probe tips on drive and on sense pads of the device.

4. Connect the current limited supply to the drive pads (with a voltmeter in parallel and a current meter in series).

5. Connect function generator and oscilloscope (in series) to the sense pads. Turn on generator at a low voltage (<0.5 volts) at a low frequency (1 kHz) with no bias [2].

6. Test frequency isolation by running through the function generator's frequency range. If signals occur on the oscilloscope, frequency limitation is detected. Reset frequency to 1 kHz [2].

7. Slowly increase the voltage on the high power supply until the signals on the oscilloscope and function generator match.

8. Run through the frequency range of the function generator, noting the half power frequency.

9. Remove voltage from the switch by reducing the high power supply back to zero.

10. Remove equipment in reverse order, ensuring that values are set back to minimums.

It is possible to note several characteristics of the switch using this method, including actuation voltage, actuation/leakage current, half power upper frequency, half power lower frequency, and AC isolation range.

Testing the "locking" switches is very similar to testing "constant" switches. All steps of testing can be duplicated with some completed out-of-order. Additionally, more

measurements can be taken for DC operation of these devices. A list of the procedures necessary for testing "locking" switches is as follows:

1. Ensure that all equipment is turned 'off' and that settings are at their minimum levels.

2. Place the die in the center of the micromanipulator table, turn on the vacuum, nitrogen, and power to the table.

3. Place probe tips on drive and sense pads of the device.

4. Connect the current limited supply to the drive pads (With a voltmeter in parallel and a current meter in series). Connect this supply through the sequencer for linear and rotational motors.

5. Connect function generator and oscilloscope (in series) to the sense pads. Turn on generator at a low voltage (<0.5 volts) at a low frequency (1 kHz) with no bias [2].

6. Test frequency isolation by running through the function generator's frequency range. If signals occur on the oscilloscope, frequency limitation is detected. Reset frequency to 1 kHz [2].

7. Actuate design until latched, remove voltage from design.

8. Run through the frequency range of the function generator, noting the half power frequencies.

9. Disconnect function generator, apply DC voltage source to closed switch.

10. Slowly increase voltage source noting both current and voltage until failure occurs.

11. Remove voltage from switch.

12. Remove equipment in reverse order, ensuring that values are set back to minimums.

Note that testing the DC characteristics of this circuit, and finding the limits thereof, is destructive and cannot be repeated on a single device. Once the maximums are found for a particular type of device, a 10% safety margin is used to test successive devices. The characteristics that can be assessed for a "locking" switch are "on" resistance, "off resistance, DC voltage and current passed, actuation voltage, actuation/leakage current, half power upper frequency, half power lower frequency, and AC isolation range.

## 4.6.    Design Descriptions

### 4.6.1.   Flip-Switch Designs.

The flip-wire switches are designed to carry a signal with a very low contact resistance. The design uses a previously designed flip-wire, used with a linear motor to make a linear switch. A three dimensional representation of the linear flip-wire switch is shown in Figure 4.4. This design was actuated by backbending the engagement actuators as seen in Figure 4.5, and applying pulsed input to the engagement and drive actuators causing the linear motor to move through its range of motion. This action brings the contact bar under both flip-wire contacts, and removes it from one contact when the motor is actuated in the opposite direction. The final design has been made such that the range of motion only extends to these two cases. Figure 4.6 shows the signals necessary to engage the switch. Reverse the polarity of the push portion of the waveform to reverse actuation direction.
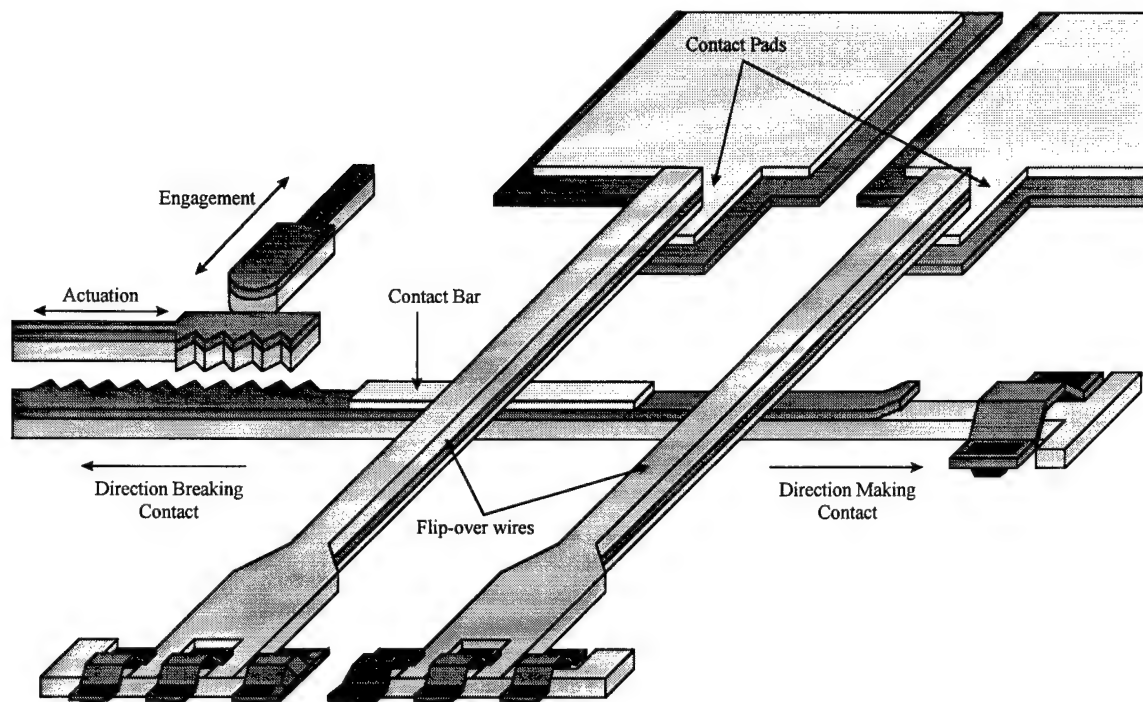
**Figure 4.4:** Linear flip-wire switch layout.
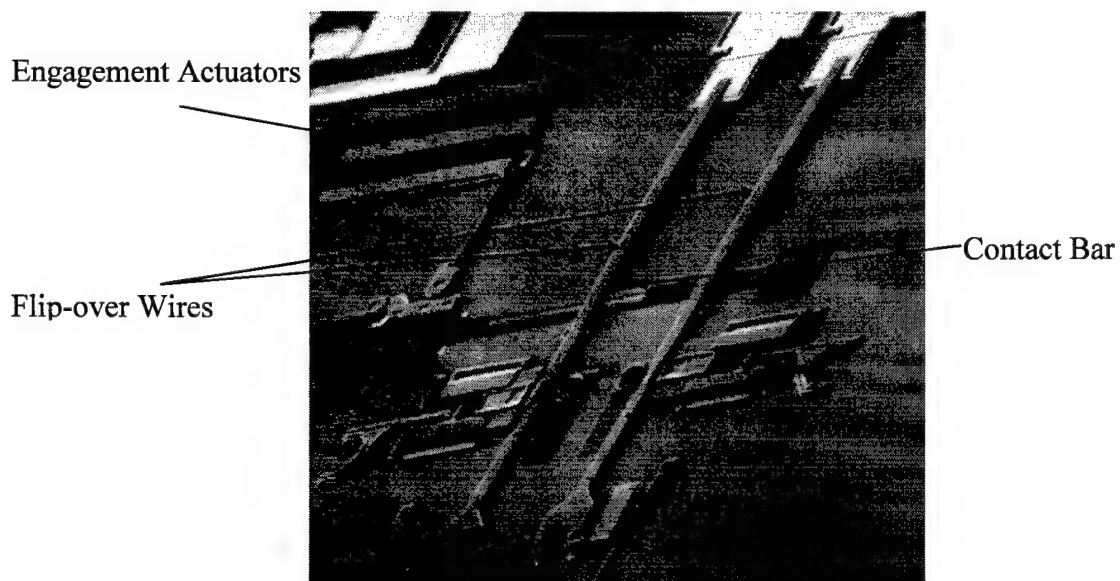


**Figure 4.5:** SEM micrograph of linear flip-wire switch.
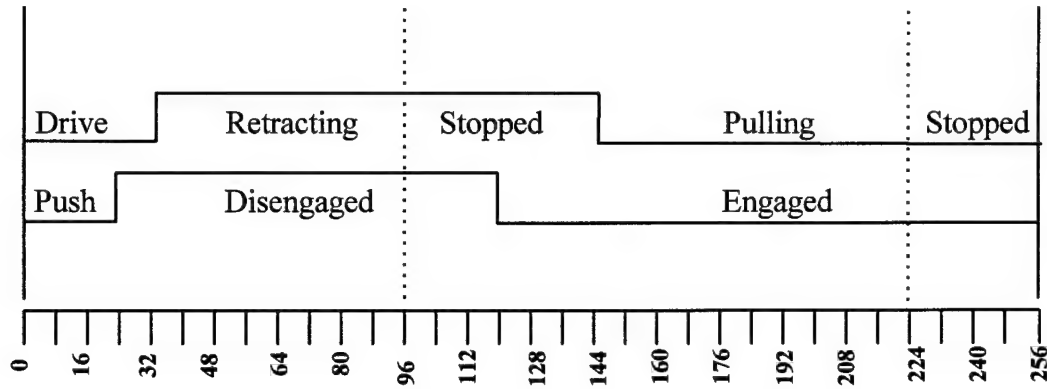
**Figure 4.6:** Waveforms for micromotors in linear flip-wire switch [18].

The motion of this device was characterized by the number of pulses necessary to actuate the design to form gold-gold contacts from the fabrication position, and the average power dissipated during the period of actuation.

### 4.6.2. Rotary Compression Switch Designs.

Rotary switches were designed to provide pressure via an increasing diameter wheel to a contact bar. This pressure caused by the expanding cylinder makes the contact connect along its edge with a stationary bar. The contact is a polysilicon-polysilicon contact, which results in a larger resistance than gold contacts. Figure 4.7 provides an overview of this structure. Actuation uses pulse trains that are implemented using the same principle as the flip-wire switch. Actuation pulses shown in Figure 4.6 will actuate this design in the counter-clockwise direction, causing the circuit to complete. Causing the push pulse to change from normally open to normally closed switching will cause the wheel to disengage the two contacts, thus breaking the circuit.
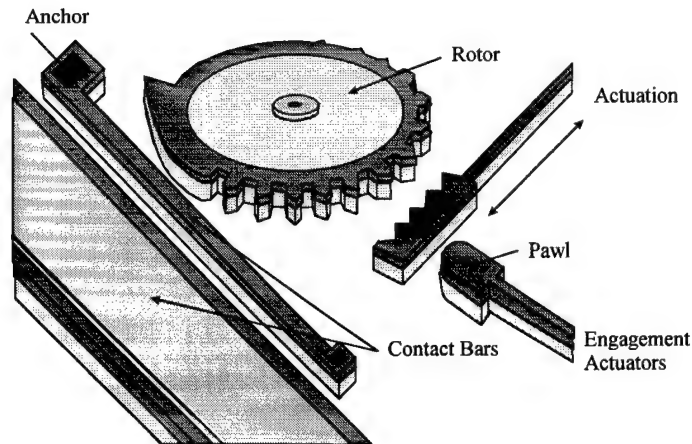
**Figure 4.7** Rotary compression switch.

Figure 4.8 shows a scanning electron micrograph of the fabricated structure. MUMPs production runs 18 and 19 used a gold based carrier for the contacts, while MUMPS 20 was designed with no gold on the contact bars to facilitate the Nickelex ™ electroless plating of the polysilicon structures.



**Figure 4.8:** Scanning electron micrograph of rotary compression switch.

### 4.6.3. Ramp Switches.

These simple latching switches, shown in Figure 4.9, use a thermal actuator array to force a contact between similar bars. This contact can be broken by a second array, and
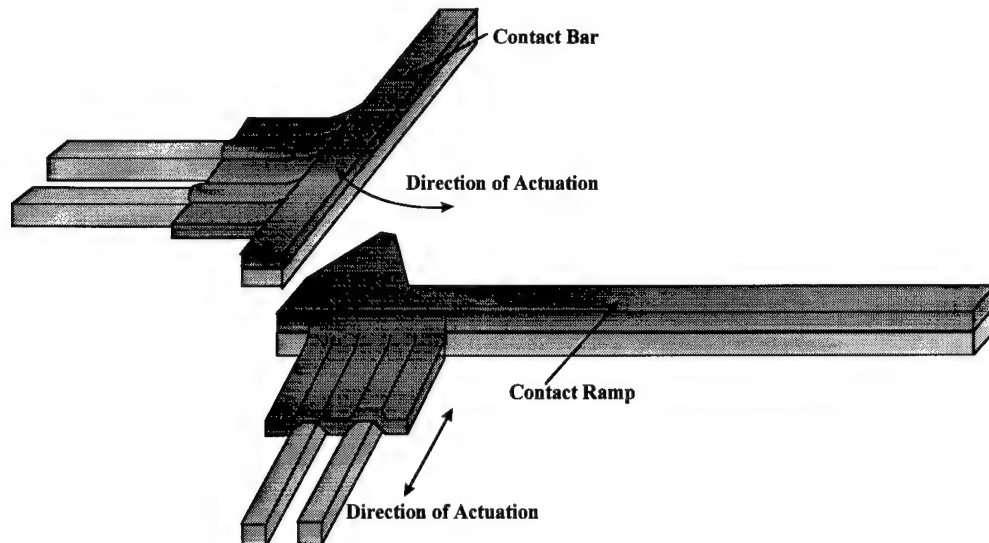


**Figure 4.9:** Ramp switch design.

used repeatedly with little effort. These devices were characterized by the amount of power necessary to actuate and contact resistance. This device was optimized for the use of Nickelex ™ electroless plating in MUMPs 20. Other versions of this design can be found in MUMPs 19 and 21. Figure 4.10 shows the MUMPs 19 implementation of the ramp switch. The contact ramp and contact bar consist of layered poly-1, poly-2 and gold. The gold in this design carries the bulk of the current, with connections being polysilicon to polysilicon. MUMPs 20 designs have no gold contact bars, but have nickel to nickel contact areas after plating.
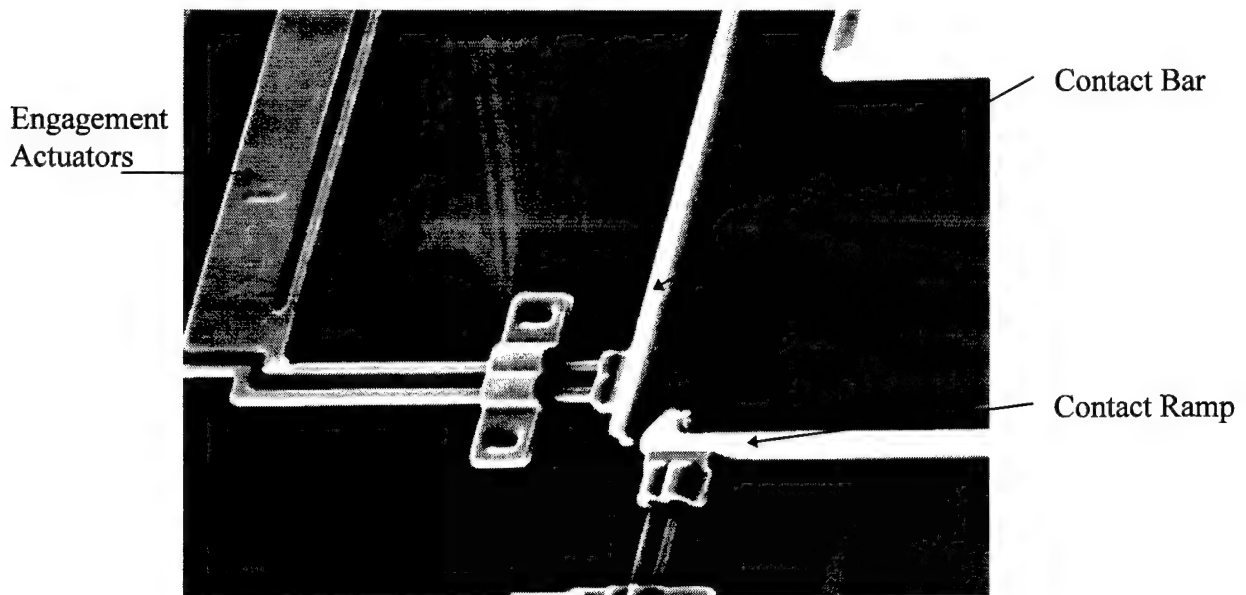
**Figure 4.10:** Scanning electron micrograph of ramp switch.

### 4.6.4. Gripper Switch Designs.

These switches are another simple latching switch design. Thermal actuators open the gripper arms seen in Figure 4.11 and the contact arm is forced into position by their
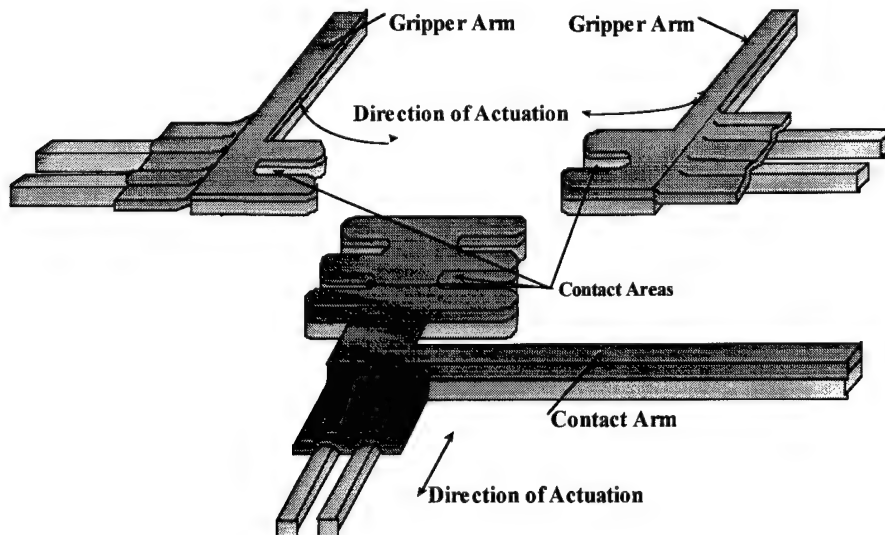


**Figure 4.11:** Gripper switch design.

thermal actuators. The gripper actuators are then released, followed by the contact arm actuators. A SEM of the gripper switch design as produced in MUMPs 19 can be seen in Figure 4.12. To release the contact, the gripper actuators are again actuated and released, freeing the contact arm.

MUMPs 19 versions of this switch are poly-1 poly-2 stacked with a gold covering layer. These designs use a polysilicon to polysilicon contact whereas the nickel plated
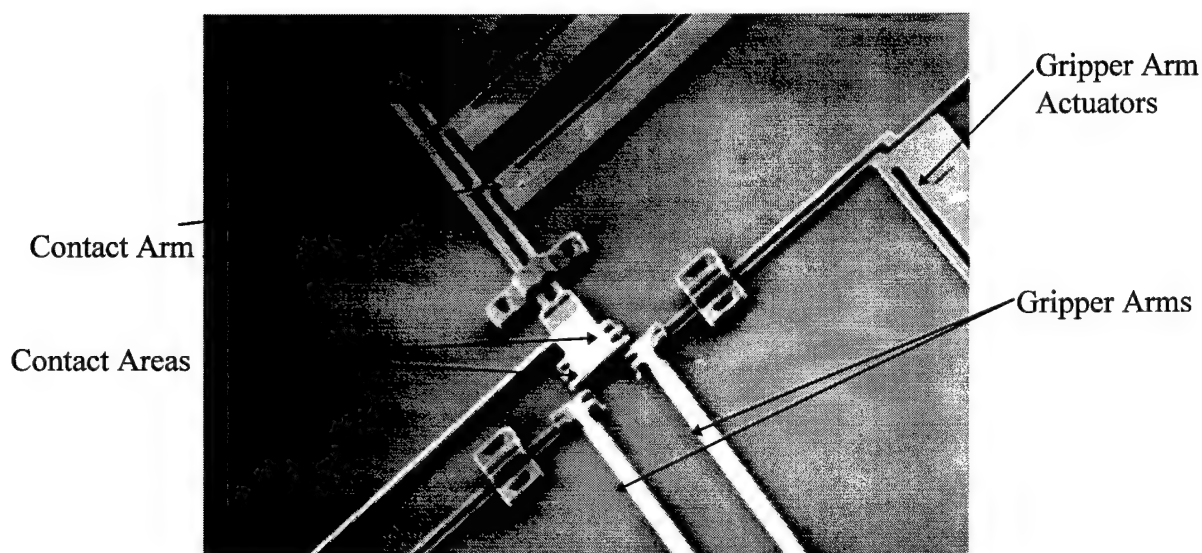


**Figure 4.12:** Scanning electron micrograph of gripper switch.

version in MUMPs 20 use a lower impedance nickel to nickel contact. The gripper switch designs were characterized by the amount of power required to open and close the contact, as well as the contact resistance.

### 4.6.5. Electrostatic Resist Designs.

These switch designs use a unique process developed as part of this thesis research. A switch with a floating plate was designed. This plate has a hole in the center that is partially released, then patterned with photoresist, hence the name "resist". The patterned

4-18

die is then completely released, causing the plate to be supported by a photoresist post as

show in Figure 4.13. The electrodes beneath the switch then pull the plate down to
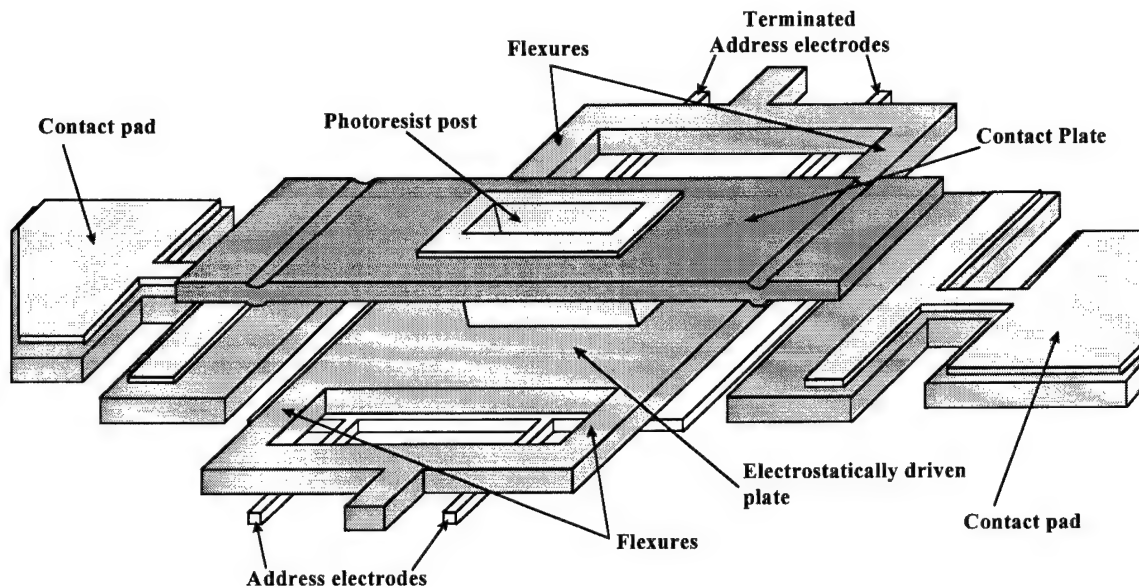
**Figure 4.13:** Electrostatic resist switch layout.
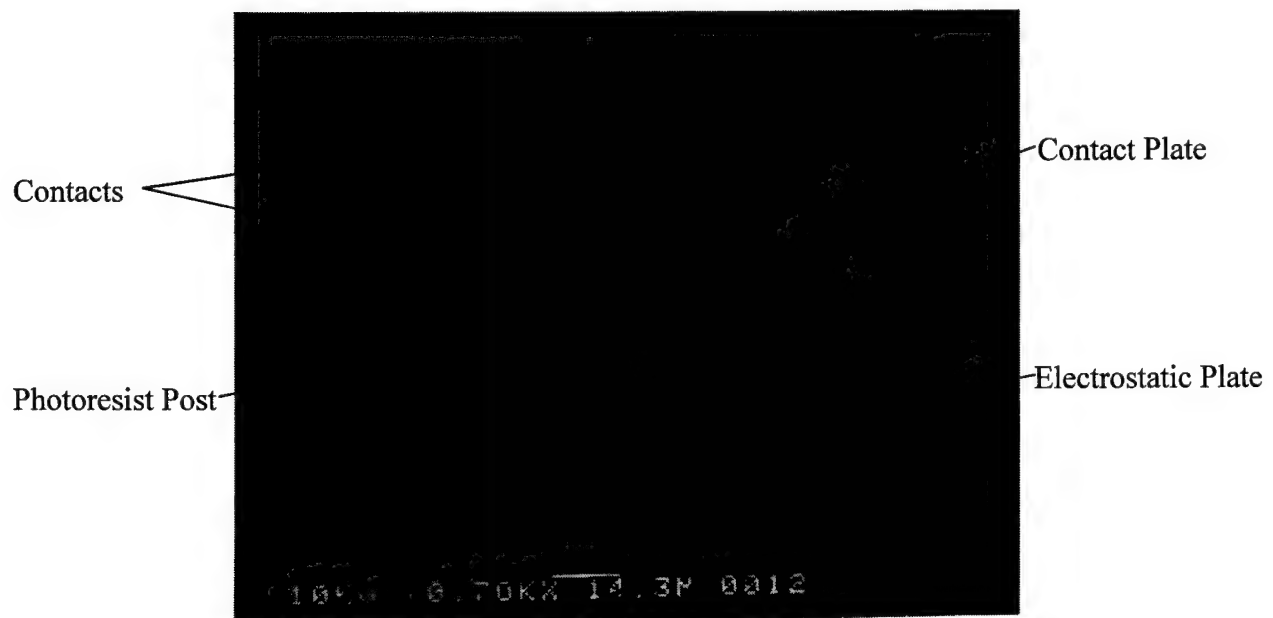
**Figure 4.14:** Electrostatic resist switch.

contact pads on either side of the device, completing the circuit. This switch is another prime Nickelex ™ plating candidate, since the switch uses a highly resistive polysilicon to polysilicon contact. A scanning electron micrograph of this switch is shown in Figure 4.14.

### 4.6.6.  Electrostatic Flip-Switch Designs.

Two different designs were constructed to act as flip-over switches. The first design, consists of an electrode with a flip-over wire connected to a substrate contact.
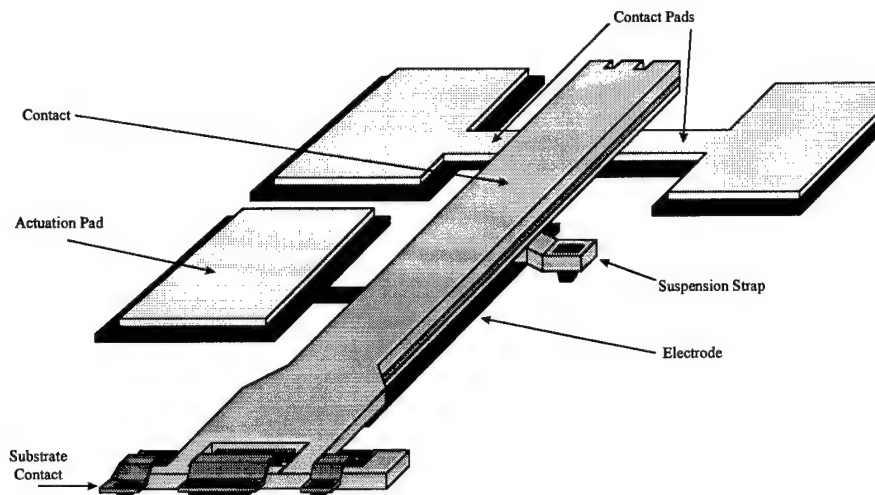


**Figure 4.15:**  Electrostatic flip-over switch with substrate contacts layout.

Figure **4.15** shows the general layout and design of this switch. A scanning electron micrograph of the fabricated design can be seen in Figure 4.16. As shown, this switch flips over to touch two gold plated contacts near the end of the switch. The flip-over wire is prevented from crashing to the substrate by a 2 μm wide strap of poly-1.

Contacts

Suspension Strap

Substrate Contact

Electrode

10KU  0.49KX 20.4M  0008
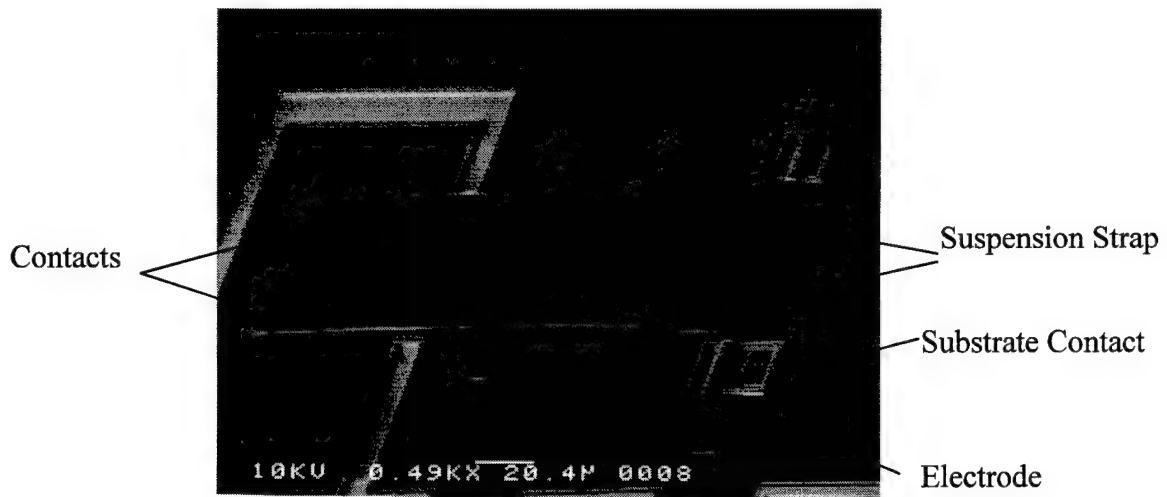
**Figure 4.16:** Electrostatic flip-over switch, substrate contacts.

The second design was implemented using a different powering scheme. A modified flip-over wire was designed to contact a gold plated pad that supplies power to the circuit. This pad, in conjunction with an electrode underneath the enlarged portion of the wire,



Contact Pads

Electrostatic
Potential Pads

Electrostatic Plate

Fixed Electrode
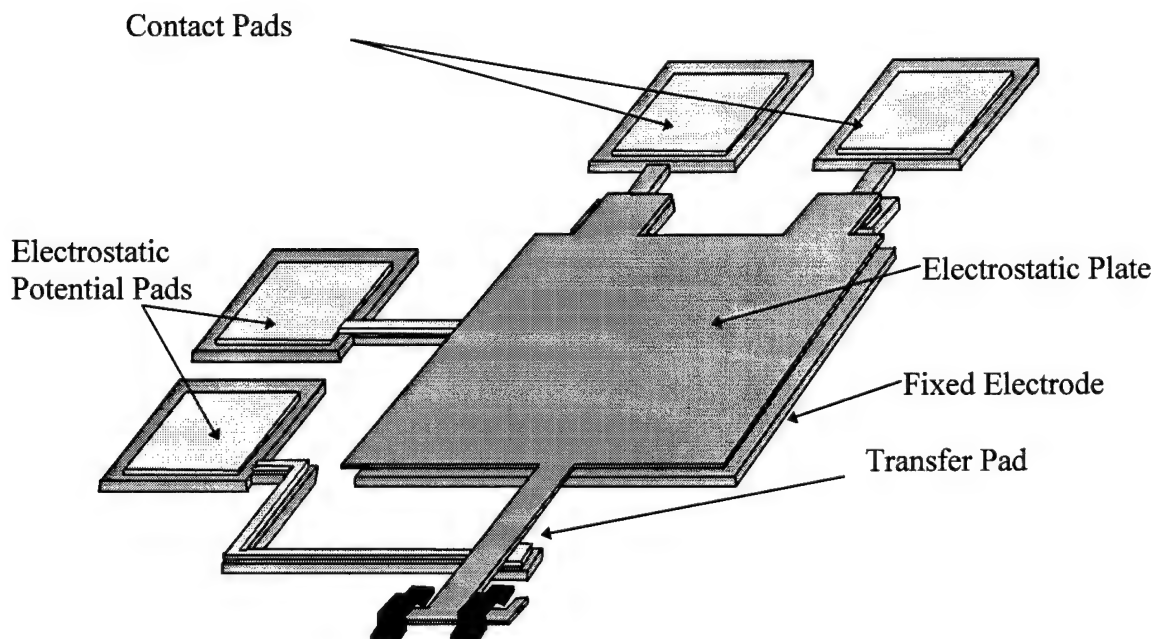
Transfer Pad

**Figure 4.17:** Electrostatic flip-over switch with transfer pad layout.

allows efficient transfer of potential between the bondpads and the device. Two trapped oxide contacts were fabricated to make a stable contact platform for this device. Figure 4.17 shows the general layout of this switch. A scanning electron micrograph of the fabricated device is shown in Figure 4.18.
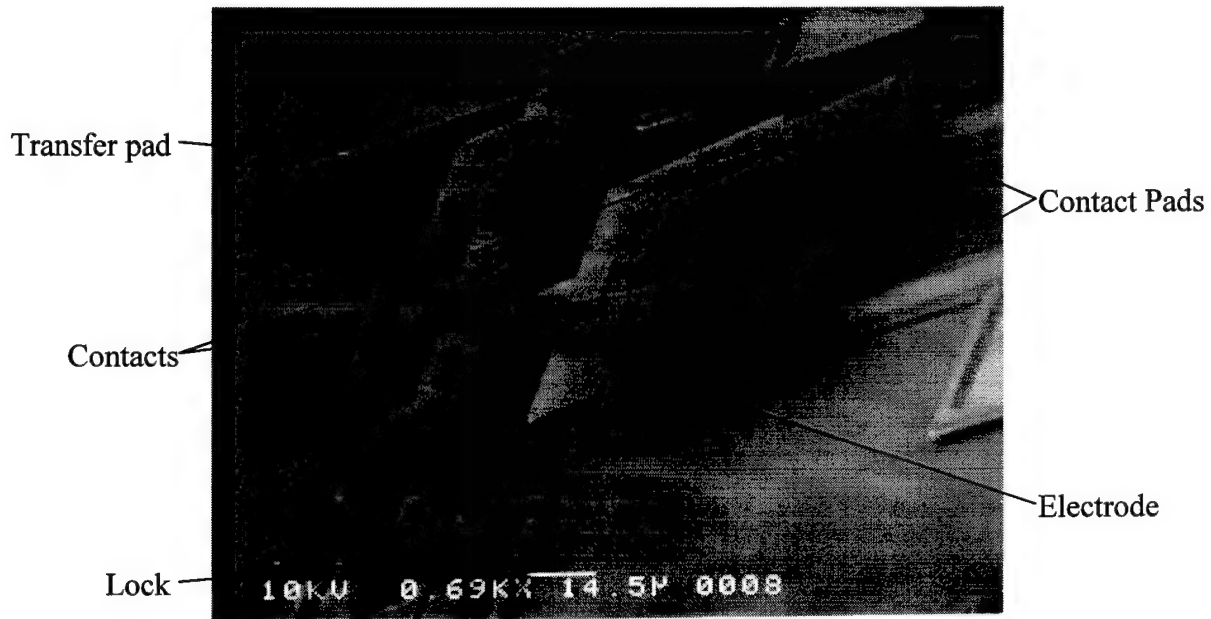


**Figure 4.18:** Electrostatic flip-over switch with transfer pad.

### 4.6.7. LIGA-MUMPs Switch

This design was originally implemented in LIGA designs and has been altered for use in the MUMPs process. The switch uses a simple thermal actuator or array of thermal actuators to latch the contact arms. The layout of this device can be seen in Figure 4.19 The arms themselves are made at the tolerance of the MUMPs process to ensure that the distance necessary to actuate is sufficiently small to use thermal actuators. Movement provided by thermal actuators can be used to actuate and deactuate the switch. The

Engagement Actuator

Disengagement Actuator
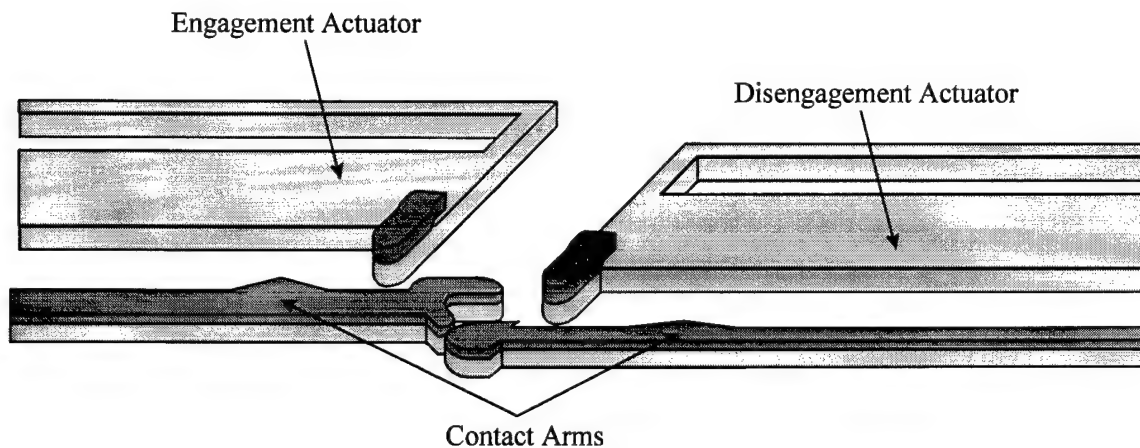
Contact Arms

**Figure 4.19:** Layout of LIGA-MUMPs switch.

design is intended to be used with the Nickelex ™ electroless plating solution to provide a low resistance contact, as designs do not include gold plating. A scanning electron micrograph of the LIGA-MUMPs switch is included in .

Engagement
Actuator

Disengagement
Actuator

Contact
Arms

10KV  1.11KX  9.01P  0013
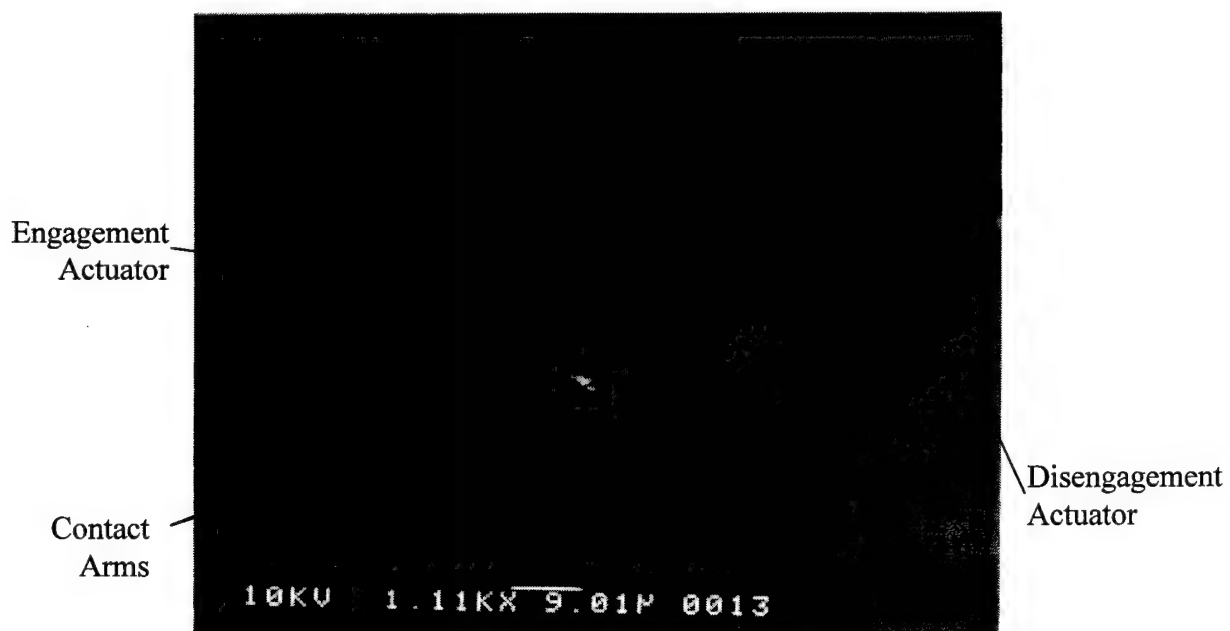
**Figure 4.20:** LIGA-MUMPs switch.

4-23

## 4.7.    *Chapter Summary*

This chapter discussed the experimental procedure and setup of this thesis.  Included were the designs that were tested, and the step-by-step method for testing.  All equipment that was required for testing purposes was annotated, along with a description of each unit's function.  Basic methodology for the MUMPs process at MCNC was discussed, as well as release procedures necessary after the individual die were shipped to the end-user.  Chapter 5 includes the data retrieved after the devices were received from the commercial foundry process (MCNC's MUMPs).

## 5. Results and Analysis

The results from the fabrication methods and testing procedures used for each switch are summarized in this chapter. First, the design results for each device on successive MUMPs submissions are detailed. The relay performance results, broken into "constant" and "latching" switch categories are discussed. Results are presented for all versions of the switches described in Chapter 4.

### 5.1. Fabrication Results

The results for the devices fabricated by the MUMPs process appear to be excellent as can be seen from the SEM micrographs of these devices. In fact, the line widths of the processes fabricated better than the tolerances suggest. Consider the micrograph
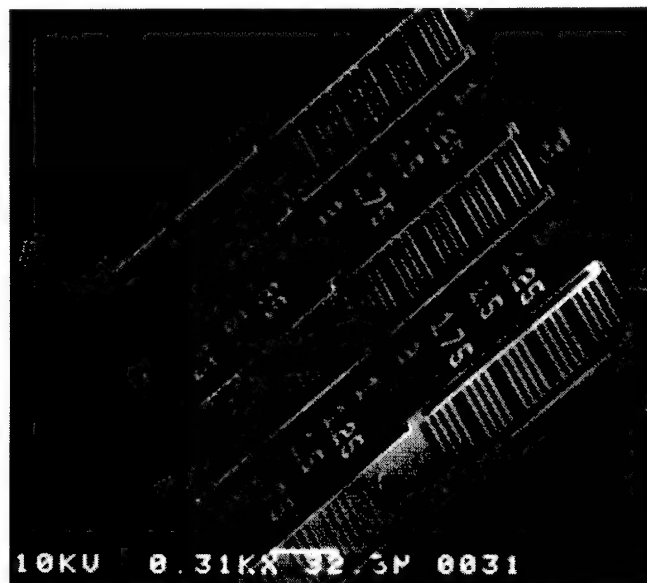


**Figure 5.1:** 45 degree line width test structure.

contained in Figure 5.1, which shows the fabrication of a 45 degree angled test structure. The minimum line widths/spaces for polysilicon are 2 μm while the minimum line width/spacing for gold is 3 μm. The poly-1 test fabricated 1 μm lines and 2 μm spaces, while the poly-2 lines fabricated to 1 μm and spaces to 1.75 μm. The metal layer (Gold/Chromium) fabricated 1 μm lines and 1.5 μm spaces. These results provide confirmation that the MUMPs process is running within specified parameters. It also follows intuitively that successive layers would have better resolution, because there are fewer processing steps to distort layers after they are deposited.

With the exception of errors made in the design of certain devices that have been discussed in Chapter 4, the devices were fabricated as expected. The SEM micrographs of the devices tested, along with the three-dimensional representations are shown so the translation from a conceptual design into a fabricated design can be observed. Enlarged three-dimensional drawings are contained in Appendix (A) while enlarged SEM micrographs are attached in Appendix (B). No major difficulties were encountered in the testing of these devices with the exception of degrading switch quality. This is due to the growth of a native oxide upon the polysilicon structures that were used as contacts in the devices.

A solution to the problem of polysilicon to polysilicon contacts on the edge of devices was to plate the devices with Nickelex™. Devices were stripped of the photoresist they were shipped in, with new photoresist spun on, patterned, and developed. The die were then immersed in a 10:1 solution of buffered hydroflouric acid for two minutes to etch away any native oxide that might have grown on the die. The now clean die were placed

into a 98° C, 500 mL bath of the Nickelex™ solution for two minutes, thirty seconds. The die were rinsed, and placed in a short methyl alcohol bath and dried. The final steps included a normal release etch in unbuffered hydroflouric acid, rinse, methyl alcohol bath, and hotplate drying.

The nickel plated upon the polysilicon structures (and gold, where exposed) grew to a 0.5 μm height according to the manual. Visual inspection showed the devices were indeed coated with a gray substance, with an irregular topology when compared to the MUMPs films. The plated film was very soft, and was easily scraped away by the probe tips of the micromanipulator station.

A second method was used to plate the die succeeding the results mentioned above. Instead of releasing the devices after plating, they were released before plating. These die had much more desirable resistance characteristics, approximately 25 Ω. The results, however were difficult to control, as the plating occurred on all sides of the polysilicon structures the solution was exposed to. In addition, the solution produced an outgassing of waste material that agitated devices to the point of destruction in several cases. Masks made to restrict exposure of the solution to contact areas must be precise as error will result in inoperative devices. Straps that hold poly-1 devices must not be exposed to the solution, as it will cause nickel to bridge the 0.75 μm gap between the two polysilicon layers.

All non-metallized relay designs designed and studied in this thesis were submitted as part of the MUMPS 20 fabrication run. The foundry provides a list of film data for each layer of the fabrication process that includes the actual thickness of each layer including

residual stresses, taken from a wafer that is fabricated on the same run as the dies themselves. Table 5.1 contains this data compiled for all three fabrication runs used in the completion of this thesis.

**Table 5.1:** Results of MUMPs 18, 19, and 20 Fabrication Data Provided by MCNC.

| MUMPs Run | Thickness (nm) | | | Sheet Resistance (Ω/□) | | | Stress (Mpa) | | |
|---|---|---|---|---|---|---|---|---|---|
| | 18 | 19 | 20 | 18 | 19 | 20 | 18 | 19 | 20 |
| Metal (Cr/Au) | 5262 | 4841 | 5250 | .0540 | .0553 | .0506 | 50(T) | 57(T) | 95(T) |
| Poly-2 | 15379 | 15384 | 14837 | 15.0 | 17.8 | 20.0 | 13(C) | 10(C) | 9(C) |
| Oxide-2 | 8032 | 7634 | 7440 | | | | | | |
| Poly-1 | 19655 | 19646 | 19428 | 9.77 | 6.9 | 10.8 | 9(C) | 10(C) | 8(C) |
| Oxide-1 | 19653 | 19293 | 19794 | | | | | | |
| Poly-0 | 5017 | 5057 | 5001 | 26.3 | 27.6 | 25.8 | 29(C) | 31(C) | 24(C) |
| Nitride | 6060 | 5695 | 5990 | | | | 160(T) | 69(T) | 132(T) |

The thickness of each layer is within the tolerances given for the foundry process for each MUMPs fabrication run. This data gives one dimension for use in the calculation of spring constants for flexures and for the force capabilities of thermal actuators. The other dimensions can be obtained from the layouts of the devices themselves.

## 5.2. *'Constant' Device Results.*

Although none of the devices fabricated in the MUMPs 19 fabrication run contained any "constant" switches, the other fabrication runs contained at least one of these devices. The devices, using either thermal or electrostatic actuation forces, include the electrostatic resist switch, the thermal bridge, and the electrostatic flip-switch.

### 5.2.1. Electrostatic Designs.

The electrostatic devices had actuation problems.  Although the devices fabricated correctly, the voltages necessary to bring them to a contact position were often excessive (>50 volts) and the devices had a very small range of movement before the electrostatic pads were slammed down to the substrate (subsequently fusing to the substrate pad).  This causes the devices to be one-use only, and not acceptable for use as relays.  The largest limiting factor in the design of these devices was the distance at which the electrodes must be placed apart for proper mechanical properties to  hold.  This relatively large distance is the primary cause for the high voltages experienced.  The secondary cause is the thickness of the polysilicon layers.  The thickness, 2.0 $\mu$m and 1.5 $\mu$m for poly-1 and poly-2, respectively, are thick enough to cause flexures made of these materials to require a large amount of force to deflect.

Electrostatic device destruction was also a problem in the course of investigation.  These devices using high voltages tend to induce large amounts of current (>100 mA) when the electrodes contact each other.  This current causes a destructive effect in the polysilicon and is seen even when using the current limiting Electrometer.  A solution has been found to this problem in the course of the investigations.  If a resistor of high enough value is placed in series with the power supply, the current can be limited to one mA.  This resistor does not affect device performance because it does not effectively limit the voltage that supplies the charge differential for the devices.  Adding this limiting resistor prevents destruction of the electrostatic devices.

### 5.2.1.1. *Electrostatic Resist Switch.*

The electrostatic resist switch uses a slightly different release method than other switches. First, a minimal etch was used to partially release the structures, leaving the contact bar suspended by unetched oxide. Photoresist is then spun on and patterned. The full release etch is then completed, leaving a post of photoresist supporting the contact bar. This process was used on two separate die to test the properties of this unique method of dielectric attachment.

The first step in testing these devices was to determine the characteristics of the electrostatic actuators that were underlying the switch components. The actuators are simple parallel plate devices attached at each end by thin flexures that ensure movement normal to the substrate. The different designs tested used different areas for the electrostatic attraction. Each device was tested to identify the voltages at which two events occurred. These events were 'movement', and 'railing'. Movement is defined as the point where the flexures are bent when viewed in a planar fashion. This describes movement normal to the substrate, because this movement causes the visible bend in the planar view of the device. The railing voltage is the point at which the device no longer returns from its actuated position. Voltages for the larger device are contained in Table 5.2, while voltages for the smaller device are contained in Table 5.3.

**Table 5.2:** Actuation Voltages For Large area device.

| Movement | "Railing" |
|----------|-----------|
| 17 V | 18 V |
| 17 V | 18 V |
| 17 V | 18 V |

**Table 5.3:** Actuation Voltages for Small Area Device.

| Movement | "Railing" |
|----------|-----------|
| 26 V | 30V |
| 27 V | 30 V |
| 27 V | 30 V |
| 27 V | 30 V |
| 27 V | 28 V |

The next step was to test the devices after the photolithography was performed. This entails determining the voltage-resistance characteristics of this device. Testing was performed on the large area devices only, as they were the only ones accurately patterned. Table 5.4 shows the results from testing these devices. Note that the voltages necessary to complete a connection in these devices is much more than the voltages necessary to implement the switches without the photoresist.

**Table 5.4:** Voltage-Resistance Characteristics for Electrostatic Photoresist Switch.

| Open Resistance | Closed Resistance | Voltage Applied |
|-----------------|-------------------|-----------------|
| ∞ | ∞ | 165 V |
| ∞ | 127 Ω | 120 V |
| ∞ | ∞ | 165 V |
| ∞ | ∞ | 165 V |
| ∞ | ∞ | 165 V |
| ∞ | ∞ | 165 V |
| ∞ | 828 Ω | 75 V |
| ∞ | ∞ | 165 V |
| ∞ | 394 Ω | 50 V |

Further examination consisted of turning over two of the patterned devices to determine the cause of so many failed contacts. On both specimens, there was a small amount of photoresist residue on the bottom of the contact areas and electrostatic plates. Since this residue is a dielectric layer, the contacts were not made on some of the devices, and possibly contributed to the high actuation voltages necessary for device actuation. The resistance values, ranging between 100 $\Omega$ and 1 K$\Omega$ are higher than a metal-on-metal contact, because the contact has to tunnel through polysilicon. The higher values seen in devices 7 and 9 are seen due to the entire path between the contacts being composed of polysilicon without a layer of gold. The smaller 100 $\Omega$ resistance is on a device that has gold on the top surface of the contact.

These devices were actuated by the electrometer, and thus current tests could not be sufficiently performed upon them. The devices operated within a range of frequencies from 100 Hz to 1 MHz with a frequency limitation of 10 MHz as defined in the experimental setup in section 4.5.

### 5.2.1.2. Electrostatic Flip-over Switches.

Two designs with variations were considered for the electrostatic flip-switch. One used a latching flip-over structure, while the other used a simpler, nitride 'sliding' flip-over structure. Actuation of both devices was attempted using the electrometer setup fix described in section 5.2.1. The voltages used in this attempt ranged from 0 to 165 volts, the maximum supply of the electrometer. As the electrometer was used, no voltage-current measurements were possible.

***Latched Electrostatic Flip-Over Switch.*** The switch, as designed, will not actuate properly. The angle at which the device assembles is too great to allow electrostatic attraction. In addition, the height of the switch is such that the latching mechanism designed to keep it in contact with its supply electrode will not work. The current two dimensional layout of the switch can be seen in
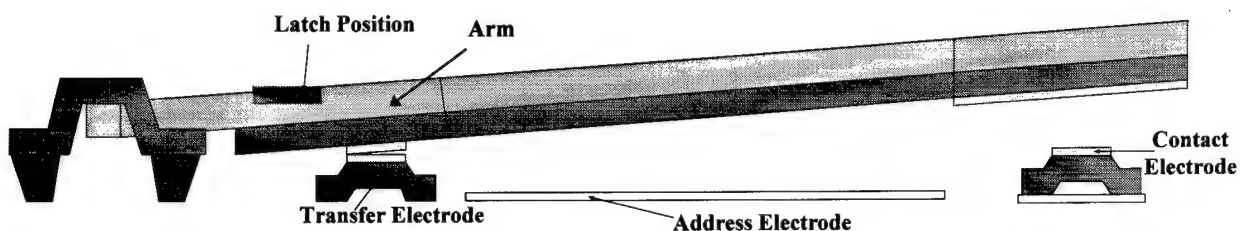


**Figure 5.2:** Side view of latching electrostatic flip-over switch.

Figure 5.2. Note that the height of the transfer electrode and the length of the arm of this switch determines the angle at which the device will be oriented relative to the substrate. The designs for this switch were not adequately spaced to provide a small enough distance between the address electrode and the electrostatic area of the switch.

Measurements for transmission characteristics including resistance, current capacity, and isolation ranges were made by forcing manual connection to the contact electrode with a probe tip from the micromanipulator. This method produces the results located in Table 5.5. A frequency limitation, defined as the frequency at which a signal can be seen upon an open switch output, can be seen in the switches. Only one case existed in this testing that did not exhibit the frequency limitation at the limit of the testing equipment's range of input frequencies.

**Table 5.5:** Characteristics of Latched Electrostatic Flip-Over Switch.

| Resistance (Ω) | Current Passed | Voltage Passed | Frequency Passed | Frequency Limitation |
|---|---|---|---|---|
| 1 | 400 mA | 6.15 V | 100MHz | 250MHz |
| 1 | 430 mA | 5.18 V | 250MHz | None. |
| 64 | 470 mA | 6.00 V | 100MHz | 250MHz |
| 5 | 450 mA | 3.05 V | 100MHz | 250MHz |

*Nitride Sliding Electrostatic Flip-Over Switch.* This switch, only implemented on the MUMPs 19 design run, had varied success. The optimum device driving parameters could not be obtained from the test samples of this device because there was no noticeable correlation between the results of the devices. The thicker devices tested measured 60 μm across by 270 μm long. These devices showed the resistance-voltage patterns as described in Table 5.6 with a standoff voltage of >165 volts.

Notice the second and sixth switches never reached closure, even at 165 volts of potential. Switches 1, 3, 4, and 5 worked to the low resistances well, not bonding to the stationary electrode due to the poly-2 strap across this pad to prevent this occurrence.

**Table 5.6:** Large nitride sliding switch voltage-resistance characteristics.

| Open Resistance | Closed Resistance | Voltage Applied | Frequency Passed | Frequency Limitation |
|---|---|---|---|---|
| ∞ | 13.3 Ω | 112 V | 10 MHz | 100 MHz |
| ∞ | ∞ | 165 V | - | - |
| ∞ | 16.2 Ω | 121 V | 10 MHz | 100 MHz |
| ∞ | 36.3 Ω | 158 V | 10 MHz | 100 MHz |
| ∞ | 93.6 Ω | 95 V | 10 MHz | 100 MHz |
| ∞ | ∞ | 165 V | - | - |

The switches that were operational showed repeatable characteristics. The rate at which these devices can be switched reached 106 KHz, which is the maximum frequency that can be applied by the testing equipment used. This rate used a 50% duty cycle square wave provided by the relay system mentioned in Section 4.4 of this thesis. Resistance measurements after several million cycles proved to be approximately 10 $\Omega$ greater, with an actuation potential required of 8 volts greater than the initial isolation. Remaining switches did not make electrical contact, even at 165 volts of potential.

The smaller switches provided much less desirable results. These switches measured 30 μm wide and 270 μm long. Only two such switches were available to be tested, with unsatisfactory results. Table 5.7 details the voltage-resistance characteristics exhibited by the smaller version of this switch. The lack of reliable resistances of these smaller

**Table 5.7:** Small Nitride Sliding Switch Voltage-Resistance Characteristics.

| Open Resistance | Closed Resistance | Voltage Applied |
|:---:|:---:|:---:|
| ∞ | 1 MΩ | 70 - 165 V |
| ∞ | ∞ | 165 V |
| ∞ | ∞ | 165 V |
| ∞ | ∞ | 165 V |
| ∞ | ∞ | 165 V |
| ∞ | ∞ | 165 V |
| ∞ | ∞ | 165 V |

switches made it unreasonable to test current and frequency characteristics as it would have skewed data toward one point in the sample space.

Results for the small version of this switch were entirely unsatisfactory, as the lowest resistance value recorded was over 1 million ohms. The high resistance is unrealistic, as

the contacts are gold-on-gold, and thus should be much lower. One possible explanation is that the electrostatic areas are not large enough to pull the switch into position over the contacts. The larger switch, however, provided reliable contacts throughout a large range of input frequencies.

### 5.2.2. *Thermal Flip-Over Wire Bridges.*

Three designs were used for the thermal bridges on the MUMPs 20 fabrication run. Two such designs are "normally open" while the third operates "normally closed". The flip-over wire thermal bridge designs are only included in one testable fabrication run, and cannot be tested properly due to a design oversight. Wires are supposed to flip over to contact pads, with an extension of the flip-over wires to be available to a latching mechanism. The design oversight caused the wires to be designed too short to be latched, and thus no operation could be observed. These switches would, however, have a high average power (power applied over time) since current on the order of tens of milliamps at 5 volts DC must be applied constantly to keep the thermal actuators driving them actuated.

### 5.3. *'Locking' Device Results.*

The 'locking' switches in this thesis are found on all MUMPs runs. These designs, working by locking a contact bar into a position and later releasing it are the heart of this research. Locking designs provide a connection that is either connected or disconnected with a very low average power consumption.

### 5.3.1. *Linear Flip-wire Switch.*

At first glance, the final version of the linear flip-wire switch seemed the most promising of all devices tested. Devices in the MUMPs 18 and 19 fabrication runs had a design oversight. The design requirement for separation between the edge of poly-2 and the poly-1 poly-2 via etch was not observed, and thus caused a separation to occur in the bar of the linear motor. This bar operates the switching of the device, and thus caused the devices fabricated to be inoperable.

Devices in MUMPs 20 were designed with the via separation requirement in mind, and fabricated flawlessly. Extra latches were also added to ensure proper force upon the contact bar of the device. The pulses described in Section 4.6.1 easily powers this switch, at a pulse peak of 7.5 volts for the primary actuator array, and 6.5 volts for the secondary actuator array. Both arrays were back bent at approximately 0.5 volts over working voltages to place them in the proper position for actuation. With the sequencer available in the laboratory, switching speeds through the entire range of motion at 2 kHz were observed with an input waveform of 100 kHz. The input waveform drives the linear motor of the switch through its range of motion. The ratio of input signal on the linear motor to switching speed is approximately 50:1. This ratio could be lowered by only operating the device within a 20 μm range instead of the full range of motion.

Initial current characteristics of this switch were outstanding! The linear flip-wire switch operated to pass up to an Ampere of current. When attempting to determine the stand-off voltage, however, it was found that there was an unintentional breach of the nitride. This caused current to be conducted through the substrate, and invalidate the

switch results. The discovery of substrate contact on the output pads prompts a change in the testing methods used for this switch. The ends of the flip-over wires are intentionally broken so that they will not contact the pads. Resistances and voltage-current characteristics is then measured from the polysilicon side of the flip-over wires. The polysilicon to polysilicon resistance is then subtracted to produce a rough estimate for resistances. Because the values were on the same order of magnitude (~170 k$\Omega$), resistances are also calculated by using a parallel resistor model through the substrate. The original values were used with a 120 $\Omega$ substrate resistance to find the correct values. The current measurements are directly measured through the polysilicon side of the wire. Standoff voltage is greater than 165 volts. Values are tabulated in Table 5.8.

Tests of the flip-over wires and contact bar were conducted to verify maximum current characteristics of the switch. The contact bar will pass 250 mA at 2.8 V DC while the flip-over wires can pass 130 mA at 1.3 V DC. Becuase the limiting factor is a 130 mA on the flip-over wires, an 82 to 115 mA maximum current is reasonable.

**Table 5.8:** Characteristics of Linear Flip-Wire Switch.

| Open Resistance | Interpolated Resistance | Voltage Applied | Current Passed | Frequency Passed | Frequency Limitation |
|---|---|---|---|---|---|
| ∞ | 15 $\Omega$ | 1.3 V | 100 mA | 10 MHz | 100 MHz |
| ∞ | 26 $\Omega$ | 2.8 V | 82 mA | 10 MHz | 100 MHz |
| ∞ | 3.0 $\Omega$ | 1.0 V | 115 mA | 12 MHz | 100 MHz |

A reliability test is performed to determine the lifetime of the switch. A switch was tested to 2,500 on/off cycles of operation. The contact bar showed no visible wear over the duration of these cycles at 850 times magnification.

### 5.3.2. *Rotary Compression Switch.*

This switch can be found in MUMPs 18 and 20. The device has good electrical characteristics when the polysilicon is slightly over metallized. There are several design problems that showed up in this switch during the course of fabrication. The first error, seen in MUMPs 18, consists of a solid polysilicon connection between both the drive and engagement actuator arrays. This connection, since both arrays have a common ground, caused leakage current to move the engagement array, disturbing the required difference between pulses of the drive and engagement arrays. The design error caused a revision to be made that removed the physical connection between the arrays. The revised arrays, based upon the design for the linear motor and implemented in MUMPs 20 and 21, use a pushing "pall" to engage the actuators to the gear. This revised array, through failure of quality control methods, ended up with the pawl disconnected from the engagement array, and thus non-operational.

The contacts of the rotary compression switch produced on the MUMPs 20 fabrication run were plated with Nickelex™ before release. The contact resistances measured for the gold plated version of this switch are shown in Table 5.9. The over-metallization is an

**Table 5.9:** Characteristics of Original Rotary Compression Switches.

| Open Resistance | Closed Resistance | Voltage Passed | Current Passed |
|---|---|---|---|
| ∞ | 4.94 kΩ | 1.2 V | 20 mA |
| ∞ | 1.26 kΩ | 1.0 V | 30 mA |
| ∞ | 225 Ω | 1.6 V | 35 mA |
| ∞ | 217 Ω | 1.7 V | 46 mA |

attempt to provide gold to gold contacts on the edge of a device rather than using a polysilicon to polysilicon contact. The different devices had similar resistance characteristics depending upon metallization which is complied in Table 5.9.

The rotary compression switches implemented in MUMPS 20 were plated with the Nickelex™ solution and proved to have unsatisfactory results. The nickel plating surface was rough, and apparently did not offer sufficient contact area when the device was

**Table 5.10:** Resistance Characteristics of Nickel Plated Rotary Compression Switch.

| Open Resistance | Closed Resistance |
|---|---|
| ∞ | 12.23 kΩ |
| ∞ | 42.8 kΩ |
| ∞ | 155.0 kΩ |
| ∞ | 8.0 MΩ |
| ∞ | 180.0 kΩ |
| ∞ | 175.0 kΩ |
| ∞ | 19.00 kΩ |

engaged. Table 5.10 shows the resistance characteristics of the plated rotary compression switches.

### 5.3.3. Ramp Switch.

The ramp switch described in Section 4.6.3 is the simplest of the switches designed for this thesis. The switch had designs to push the envelope of the MUMPs process. The designs for the MUMPs 19 fabrication run allowed for a 2 μm gap between the contact ramp and bar. The devices fabricated well at the 1.5 μm gap, and were carried into the MUMPs 20 fabrication run without metallization. Table 5.11 shows the resistance characteristics of the metallized switches on the MUMPs 19 lot. The different fabrication

widths did not have a bearing on the resistance, because the ranges were identical for both widths. Devices on this lot were inadvertently designed with the thermal actuator arrays backward, and thus were not able to be actuated as intended.

**Table 5.11:** Resistance Characteristics of Ramp Switch.

| Open Resistance | Closed Resistance |
|---|---|
| $\infty$ | 51.7 k$\Omega$ |
| $\infty$ | 68.6 k$\Omega$ |
| $\infty$ | 55.2 k$\Omega$ |
| $\infty$ | 2.01M$\Omega$ |
| $\infty$ | 178.0 k$\Omega$ |
| $\infty$ | 41.4 k$\Omega$ |
| $\infty$ | 422 $\Omega$ |
| $\infty$ | 98 $\Omega$ |

The devices on MUMPs 20 were fabricated without metallization, were patterned on the same die as the rotary compression switches, and bathed in the Nickelex™ solution. These devices had no noticeable contact when actuated. The resistances were too high to be measured by the equipment in the laboratory and can be assumed infinite, or open connections. In addition, one of the errors found on MUMPs 19 propagated through to this design, causing the actuator array attached to the contact bar to remain oriented in the opposite direction than desired for operation. This was worked around by using the back-bending characteristics of polysilicon actuators to make the device a one time use latch. The process was repeatable, and performed on six different devices without incident.

### 5.3.4. Gripper Switch.

Several different design variations of the gripper switch were implemented in the MUMPs 19 fabrication run. The designs implemented varied the distance between the gripper arms and the contact arm. The distances varied between 4 µm, a safe distance for the fabrication of the gold line widths, to 2 µm, the minimum spacing for polysilicon structures. A variation of the number of actuators was also implemented on the device with a 2 µm gap. This variation was later implemented in the MUMPs 20 fabrication run without metal for Nickelex™ plating. The original designs on MUMPs 19 could not be tested for functionality, since the wiring that connected the gripper arms together was flawed. These devices were, however, tested for resistance and frequency characteristics as well as power dissipation while manually actuated to the closed position. Table 5.12 shows the resistance characteristics for the left and right gripper arm to the contact arm for each different design.

**Table 5.12:** Resistance Characteristics for Metallized Gripper Switch Designs.

| 2.0 µm Gap | | 2.5 µm Gap | | 3.0 µm Gap | |
|---|---|---|---|---|---|
| Left Resistance | Right Resistance | Left Resistance | Right Resistance | Left Resistance | Right Resistance |
| 1.04 kΩ | 62 Ω | 6.61 kΩ | 6.72 kΩ | 1.29 kΩ | 1.14 kΩ |
| 6.72 kΩ | 77 Ω | 5.64 kΩ | 6.76 kΩ | 394 Ω | 653 Ω |
| 6.25 kΩ | 51.4 Ω | 6.50 kΩ | 6.39 kΩ | ∞ | ∞ |
| 2.0 µm Gap Large Gang | | 3.5 µm Gap | | 4.0 µm Gap | |
| 6.50 kΩ | 6.55 kΩ | 6.62 kΩ | 6.68 kΩ | 975 Ω | 1.12 kΩ |
| 6.05 kΩ | 6.39 kΩ | 5.60 kΩ | 5.60 kΩ | 500 Ω | 45 Ω |
| 6.32 kΩ | 6.44 kΩ | 5.60 kΩ | 5.70 kΩ | 850 Ω | 140 Ω |

The data in Table 5.12 reflect a varied resistance both within a set of similar devices, and across the different device versions. The best resistances were seen from the right gripper arm to the contact arm when the devices were fabricated at 2 μm apart. Frequencies range from DC to 100 kHz with a frequency limitation of 1 MHz was noted with these devices as well. Flexures passed up to 65 mW before burning out. Note the



**Figure 5.3:** Non planarized gripper switch from MUMPs 19.

variance between these devices can be attributed to the way in which they released. Figure 5.3 shows a device that is not planarized, and is thus not making a good gold to gold contact on the top 50 μm of the device. Figure 5.4 shows the proper planarization for a reliable contact of the gripper switches in this thesis.

The "streamers" seen on these SEM micrographs are the result of over-metallization in the MUMPs process. This was intentional to possibly induce metal deposition upon the edges of the poly-2 portions of the structure. Care was necessary when manually

actuating these devices to ensure that the streamers were not in contact with other parts of the switch.

MUMPs 20 devices were made with no metal on the gripper and contact arms. The design carried over was the 2 μm gap with a large actuator array. When actuated during testing (and before plating), it was found that the drive of the actuator arrays was not
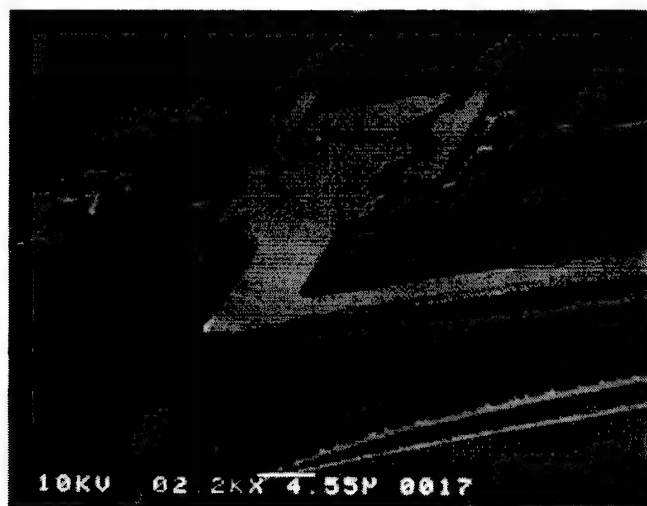


**Figure 5.4:** Planarized gripper switch from MUMPs 19.

sufficient to provide enough deflection for locking actuation. Several attempts were made that resulted in intermittent contact while never completely locking into place.

The gripper switches that were not metallized were patterned on the same die as the rotary compression switches, and bathed in the Nickelex™ solution. These devices had results comparable with the ramp switches that were plated, having no noticeable contact when actuated. The resistances were too high to be measured by the equipment in the laboratory and can be assumed infinite, or open connections.

## 5.4. Chapter Summary

This section discussed the results obtained during the course of this thesis. Included were discussions of each device fabricated, with characteristics for each device given for resistance, current capacity, and frequency ranges. Devices were marked according to their functionality under all testing situations. Nickelex™ electroless plating of three devices was also discussed, including both process and contact characteristic results.

## 6. Summary, Recommendations, and Conclusions

The research contained in this thesis has produced characterizations of several MEMS switches. This chapter contains a summary of the findings of this research by highlighting the most significant observations concerning the design, fabrication, and testing of these switches. Several suggested improvements and future research ideas are also presented.

### 6.1. Thesis Summary

In the design of micro-electromechanical switches, it is important to keep several considerations in mind that affect the capacity and performance of the devices. It was found that certain design rules, specifically via limitations, were imperative to the proper fabrication of the devices. Inattention to this rule can cause catastrophic effects upon device performance. Special attention must also be paid to topological effects. Layers that have been deposited in a non-planarizing process like MCNC's MUMPs cause successive layers to conform to the surface topology of the previous layer. This can be taken advantage of in the fabrication of hinges, but could prove deleterious in the design of devices such as micromirrors.

The primary concern in designing micro-electromechanical switches is the desire to achieve a low impedance contact that will conduct a large amount of current to the intended target. The voltage required should be low when integrating with CMOS electronics, and the power consumed over time should be kept low to preserve the lifetime of a finite power supply such as a battery. Stability of the devices is necessary to

6-1

provide a reliable contact, while isolation is required to ensure that no leakage is transmitted in the device. To this end, the locking switches were made to ensure a stable contact with the shortest possible actuation time, reducing leakage current and maximizing contact quality.

The switches studied in this thesis were fabricated by the commercial foundry at MCNC using the ARPA-sponsored MUMPs process fabrication service. This process allows one polysilicon address layer (poly-0), two releasable polysilicon layers (poly-1 and poly-2) with silicon dioxide as a sacrificial material layer. These layers are built an initial dielectric layer of silicon nitride has been deposited to isolate the silicon substrate. All devices designed during the course of this research fabricated were excellent, and performed exactly as designed. The exceptions to proper operation came due to design errors, not discontinuities in the foundry process.

The experimental setup used to measure the characteristics of the devices in this thesis worked well such that all devices were able to be characterized. The devices were able to be actuated by the equipment available, with no problems created due to the system setup viewable. This setup allowed all devices to be characterized according to impedance characteristics, frequency ranges and limitations, and power throughput. Although some devices were not operational, most provided at least some valuable information concerning operational characteristics.

## 6.2. Recommendations

Of the devices developed during the course of this thesis, only two have proven sufficient to recommend for use in a micro-satellite. The nitride sliding electrostatic flip-over switch (large version) is promising for a capable, high speed switching circuit. The linear flip-wire switch is a reasonable conductor with properties that will ensure its lifetime in such an application.

The linear flip-wire switch would be particularly applicable to those needs which include operation around 5 volts, with a high power throughput requirement, approaching 0.1 watts. The switch must be laboriously hand-assembled, however, and can be easily broken while doing so. The electrostatic nitride sliding flip-over switch, on the other hand can be used in situations where power is at a premium and voltages are high. Assembly of this switch is relatively simple, and can be done with minimal breakage.

## 6.3. Suggested Improvements

After over a year of research in the design and operation of micro-electromechanical switches, it has become evident that certain designs are better suited for operation in the MEMS arena. The expertise gained throughout the completion of this research must be passed to succeeding researchers to ensure a net increase in the corporate knowledge, to ensure that work is not duplicated. Suggested improvements provide an avenue to pass on this expertise as a foundation to future engineers.

### 6.3.1.  Better Test Equipment

One of the main avenues of improvement in the future would be improving the reliability and consistency of measurements. The micromanipulator probe station used is only accurate on measurements to approximately $\pm15$ $\Omega$. This inaccuracy is significant in testing devices that are on the same order of magnitude as the error.  Long lead lines on this station add in background noise to the signals passed and cloud normal observations.

In addition, the function generator available for testing used only discrete time steps. A generator that allows continuous settings for frequency would allow a more accurate estimation of frequency ranges and frequency limitation.

### 6.3.2.  Design Improvements

There are several improvements that can be added to the devices investigated during the course of this research.  Most of the improvements stem from design deficiencies in the original MUMPs fabrication runs.  Some of these design improvements are very simple, while others cause a severe redesign of the devices.

A very simple redesign can be implemented on the ramp switch to make it operational. Simply reversing the direction of actuation for the actuators attached to the contact bar will correct the deficiency.  The gripper switch can be corrected by putting a balanced array of the new double hot arm actuators that have been developed at AFIT onto the contact arm.  The rotary compression switches can be corrected by extending the poly-1 bar completely out to the pawl to ensure connection.  The flip-over wire bridges can be tested properly by extending the flip-over wires sufficiently to be latched.

The latched electrostatic flip-over switch bears more careful consideration than the others. The design must be redesigned to compensate for the latch in it's geometry. First, reduce the transfer pad height to 2.0 μm, then reduce the contact pads to 2.75 μm by eliminating the poly-0 former. The length of the arm should be increased, and the composition changed to poly-2 from stacked to reduce the force necessary to bend the flexure. Finally, the transfer pad must be situated such that the contacts are positioned slightly above their respective pads, approximately 5 μm.

The linear flip-wire switch must have a minor redesign to ensure the ability to properly test the device. The contact pads must be redesigned to remove the unintentional substrate contacts that were introduced through a design error.

## 6.4. Suggested Future Research

Within the Air Force, and specifically AFIT, assignment of resources to a task is daunting. Research must be in the interests of some gaining agency within the Air Force community, and those interests greatly outnumber the number of resources available. This chapter highlights suggested research that is considered important should research into these devices be continued in the future.

### 6.4.1. New Device Possibilities

Throughout this research, new possibilities in micro-electromechanical switches have been breached by myself, along with many of my colleagues. These switches range from electrostatic to discretely driven thermal actuated designs. More ideas form each day for devices that will bridge the gap to simple, reliable performance.

A design based upon electrostatics can be made by assembling three flip-up plates, two of which are fixed. One plate lies in the middle as shown in Figure 6.1, while another acts as an electrostatic attractor, and the other a second contact point. The plates can be made hundreds of microns tall, with a several hundred micron length to allow for maximum attraction area.
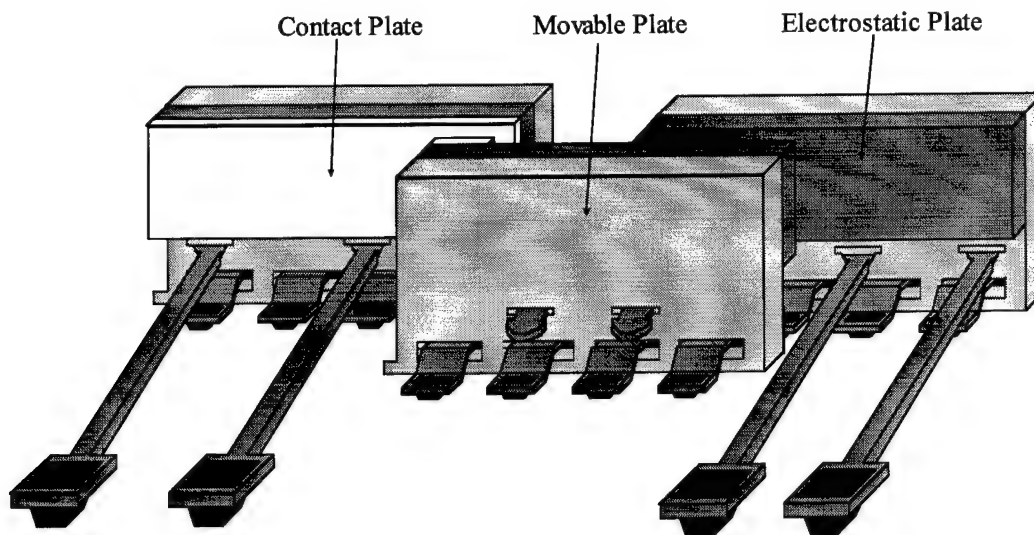


**Figure 6.1:** Vertical electrostatically actuated switch.

This design can be improved by adding a substrate sliding hinge on the movable plate, to allow for movement parallel to the substrate.

A second design consists of two large contacts, one stationary, the other movable. The movable switch can be engaged by a linear motor, and kept in place by a set of ratchets. To release the switch, the ratchets can be released, and the switch returns to it's normally open position as shown in Figure 6.2. Operation is intended to be simple, allowing for a very large contact area that should minimize impedance of the switch. A flexible wire

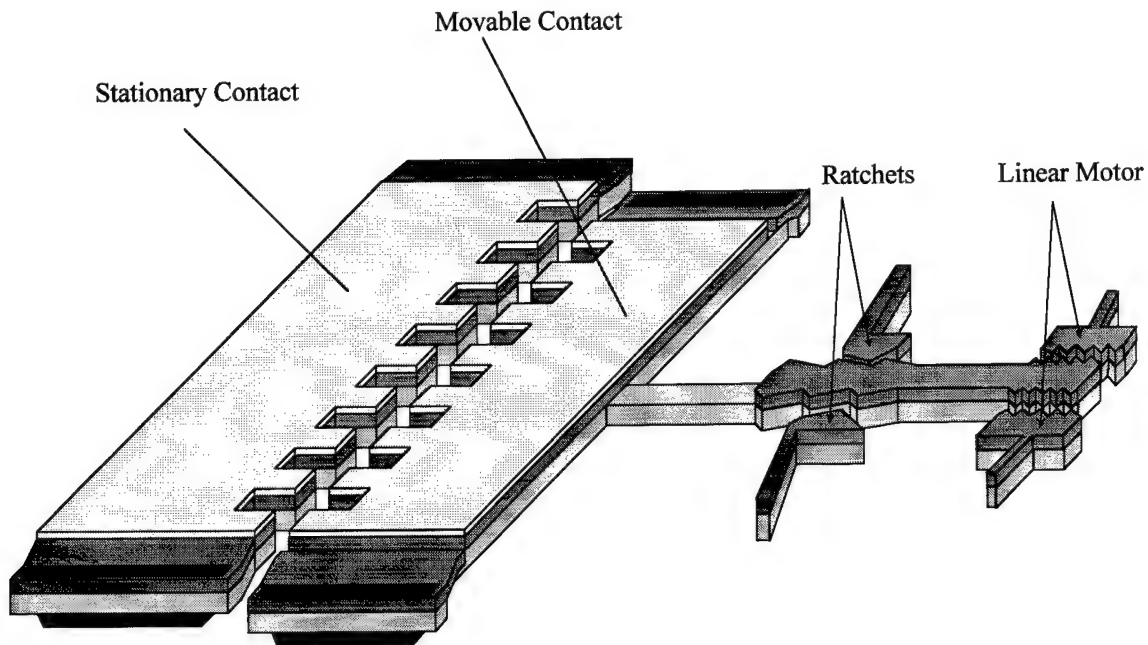should be used to connect the movable contact to act as a spring, and provide a path to ground for the switch.

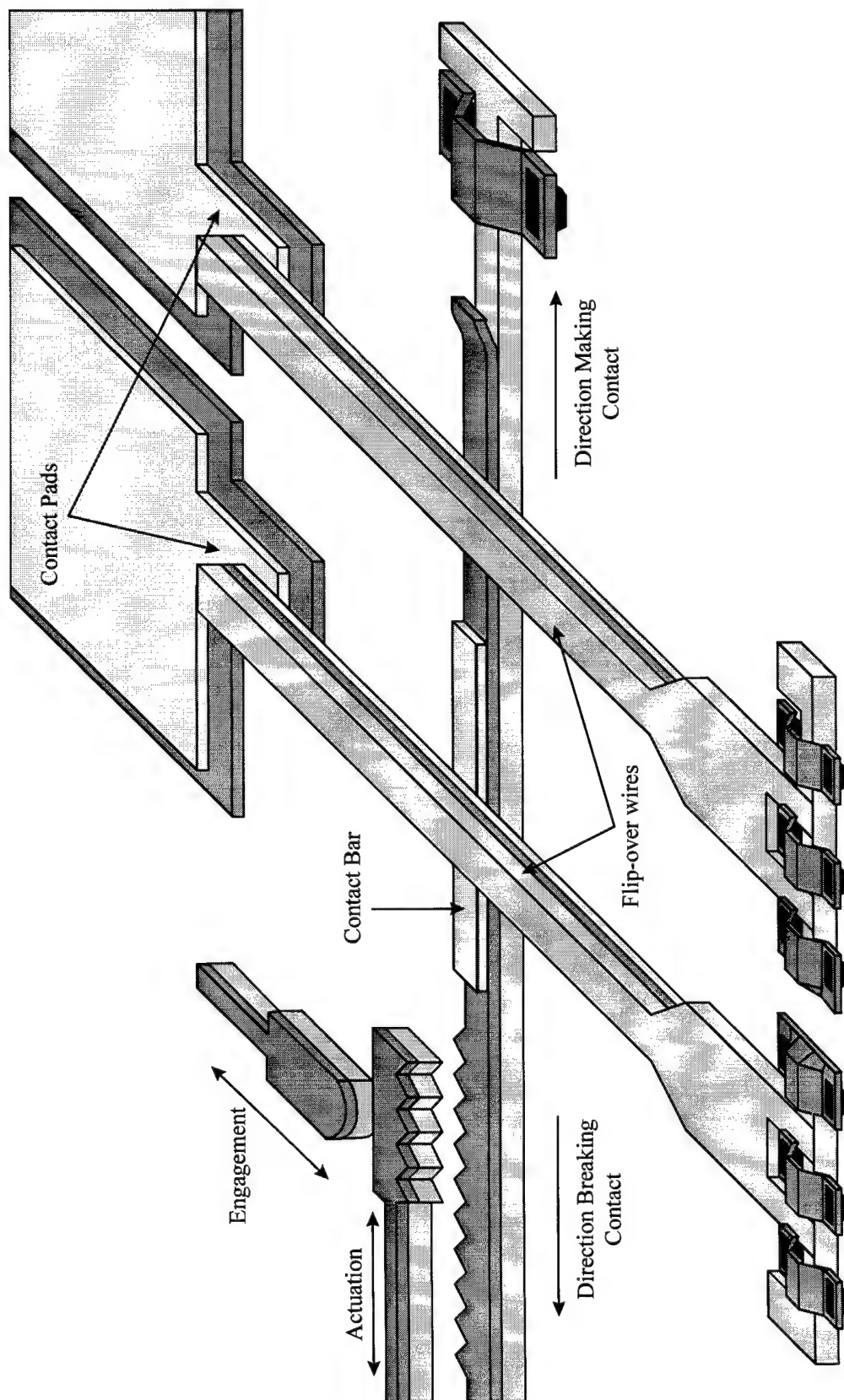Figure 6.2:  Thermally actuated ratchet switch.

## 6.5.    *Chapter Summary*

This chapter has presented a summary of the work included in this thesis, and has given recommendations to the sponsor agency.  These recommendations encompass designs that are viable for use in space based micro-satellite systems.  Recommendations have been made for improvements to existing designs and testing procedures.  Finally, the chapter presented new ideas for continued work in the field of micro-electromechanical switches.
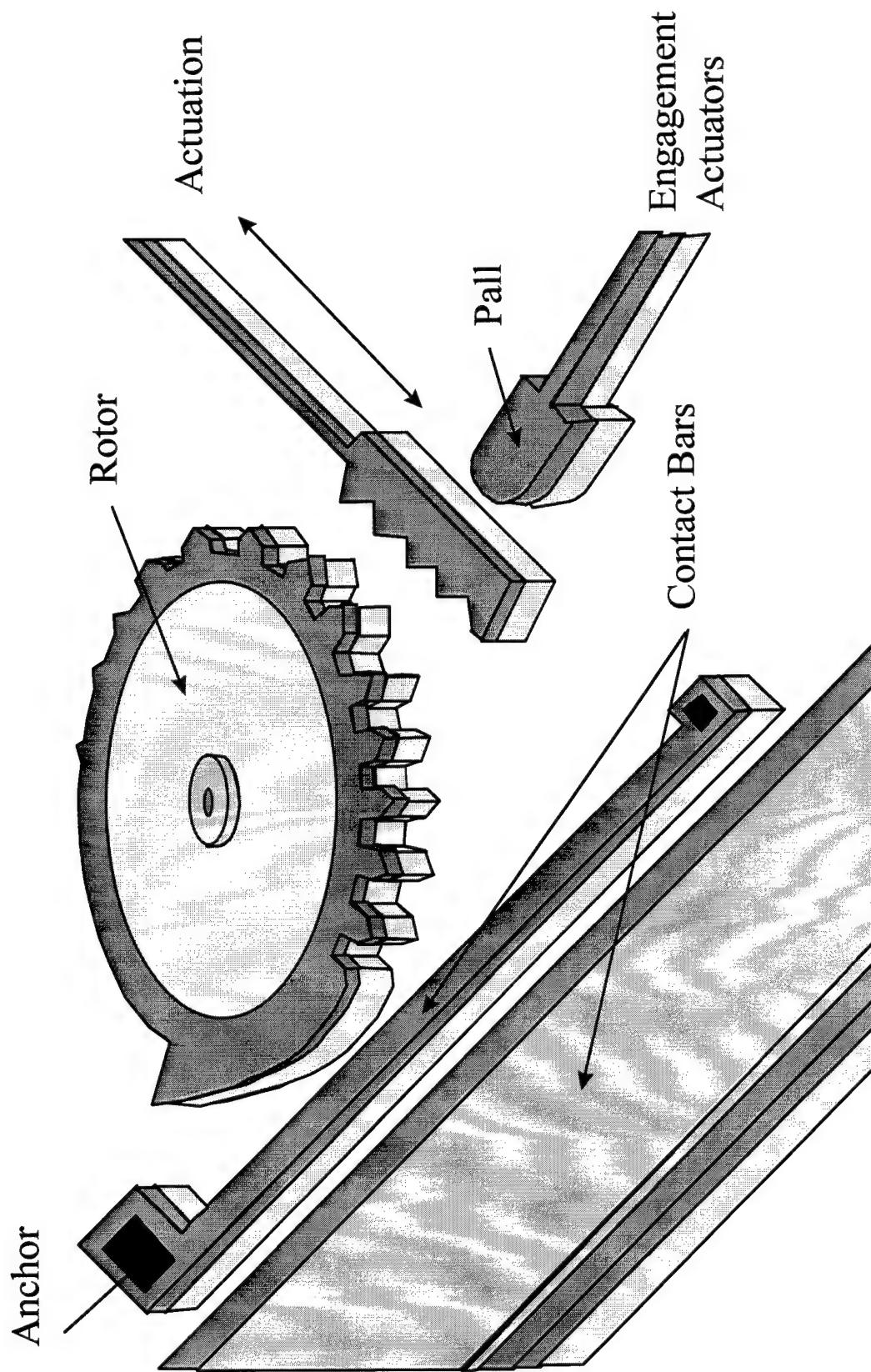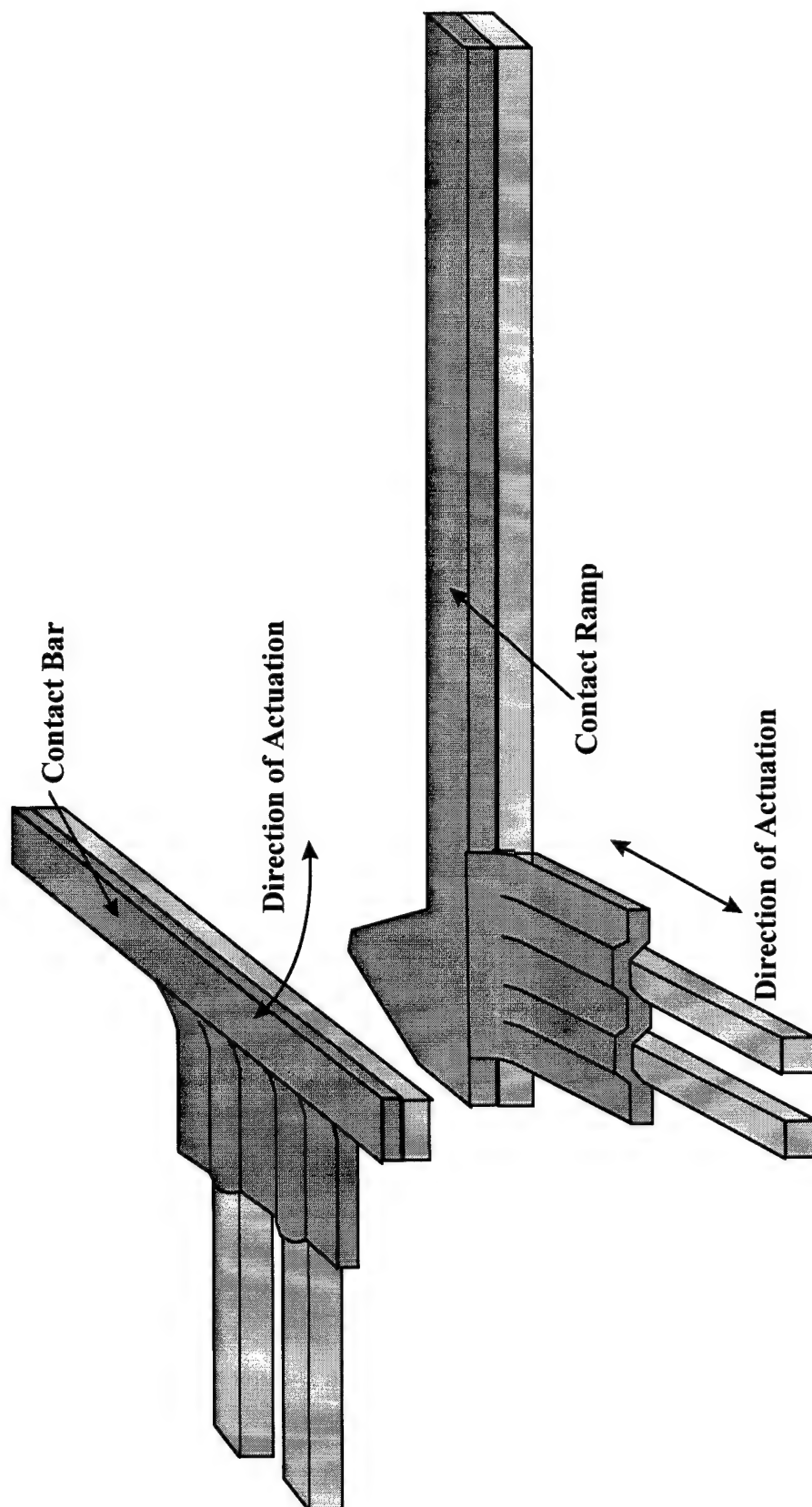
# References

[1]  H. Hosaka and H. Kuwano, "Design and fabrication of miniature relay matrix and investigation of electromechanical interference in multi-actuator systems," in *Proc. IEEE 1994 Conference on Microelectromechanical Systems*, Salt Lake City, UT, 1994, pp. 313-318.

[2]  M. W. Phipps, "Design and development of microswitches for micro-electromechanical relay matrices," Master's thesis, Air Force Institute of Technology, June 1995. (AFIT/GE/ENG/95J-02)

[3]  D. A. Koester, R. Mahadevan, A. Shishkoff, and K. W. Markus, *SmartMUMPs Design Handbook including MUMPs Introduction and Design Rules (rev. 4)*, MCNC, Research Triangle Park, NC, 1996.

[4]  J. P. Lockwood, *Applying precision switches*, Illinois: MICRO SWITCH, a division of Honneywell, 1972.

[5]  P. M. Zavracky, S. Majumder, and N. E. McGruer, "Micromechanical switches fabricated using nickel surface micromachining," *Journal of Microelectromechanical Systems*, vol. 6, no. 1, pp. 3-9, 1 March 1997.

[6]  H. Hosaka, H. Kuwano, and K. Yanagisawa, "Electromagnetic microrelays: Concepts and fundamental characteristics," in *Proc. IEEE 1993 Conference on Microelectromechanical Systems*, Salt Lake City, UT, 1993, pp. 12-17.

[7]  A. Benitez, J. Esteve, and J. Bausells, "Bulk silicon microelectromechanical devices fabricated from commercial bonded and etched-back silicon-on-insulator substrates," *Sensors and Actuators*, A 50, pp. 99-103, September 1995.

[8]  M. A. Gretillat, P. Thiebaud, N. F. deRooij, and C. Linder, "Electrostatic polysilicon microrelays integrated with MOSFETs," in *Proc. IEEE 1994 Conference on Microelectromechanical Systems*, Salt Lake City, UT, 1994, pp. 97-101.

[9]  J. Simon, S. Saffer, and C. Kim, "A micromechanical relay with a thermally driven mercury micro-drop," in *Proc IEEE MEMS Workshop '96*, San Diego, CA, 1996, pp. 515-520.

[10] A. D. Johnson and E. J. Shahoian, "Recent progress in thin film shape memory microactuators," in *Proc IEEE 1995 Conference on Microelectromechanical Systems*, Salt Lake City, UT, 1995, pp. 216.
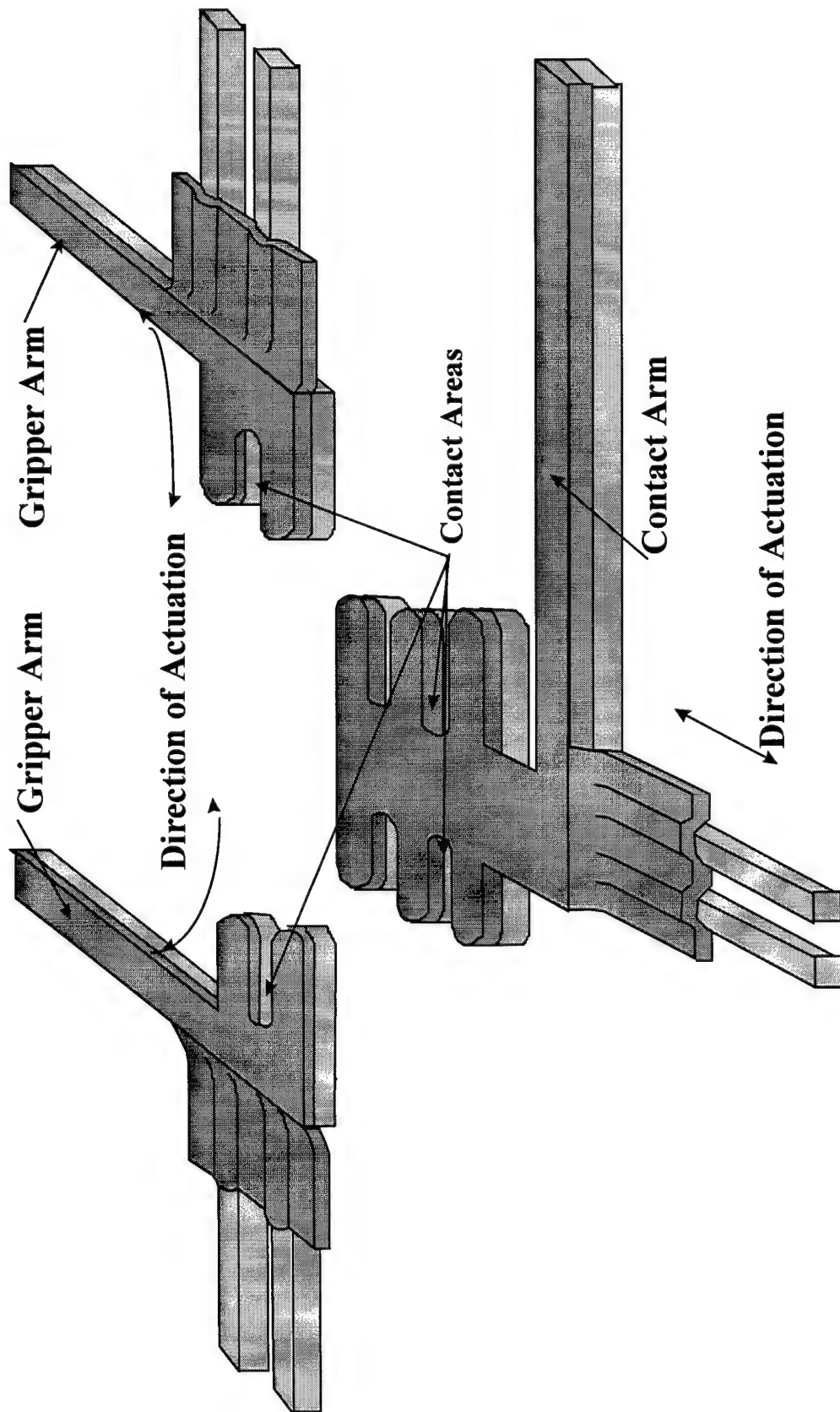
[11] W. Griffel, *Handbook of Formulas for Stress and Strain,* New York, NY: Frederick Ungar Publishing Co., 1966.

[12] M. A. Michalacek, "Design, Fabrication, Modeling, and Testing of Surface-Micromachined Micromirror Devices," Master's thesis, Air Force Institute of Technology, June 1995. (AFIT/GE/ENG/95J-01)

[13] P. Lorrain, D. R. Corson, and F. Lorrain. *Electromagnetic Fields and Waves.* 3$^{rd}$ Ed. W. H. Freeman and Company, New York, 1986.

[14] H. Guckel, J. Klein, T. Cristeson, K. Skrobis, M. Laudon, E. G. Lovell, "Thermo-magnetic metal flexure actuators," *in Proceedings of Transducers '92,* San Francisco, pp. 73-75, June 1992.

[15] J. R. Reid, V. M. Bright, and J. H. Comtois, "Force measurements of polysilicon thermal micro-actuators," *Proc. SPIE: Micromachined Devices and Components II,* vol. 2882, pp. 296-306, October 1996.

[16] J. T. Butler, V. M. Bright, and W. D. Cowan, "SPICE Modeling of Polysilicon Thermal Actuators," *Proc. SPIE,* vol. 3224, pp284-293, 29 September 1997.

[17] R. A. Serway, *Physics for Scientists & Engineers with Modern Physics* 2$^{nd}$ Ed.. Philadelphia: Saunders College Publishing, 1986.

[18] J. H. Comtois, "Structures and Techniques for Implementing and Packaging Complex, Large Scale Microelectromechanical Systems Using Foundary Fabrication Processes," Doctoral Dissertation, Air Force Institute of Technology, June 1996. (AFIT/DS/ENG/96-04)
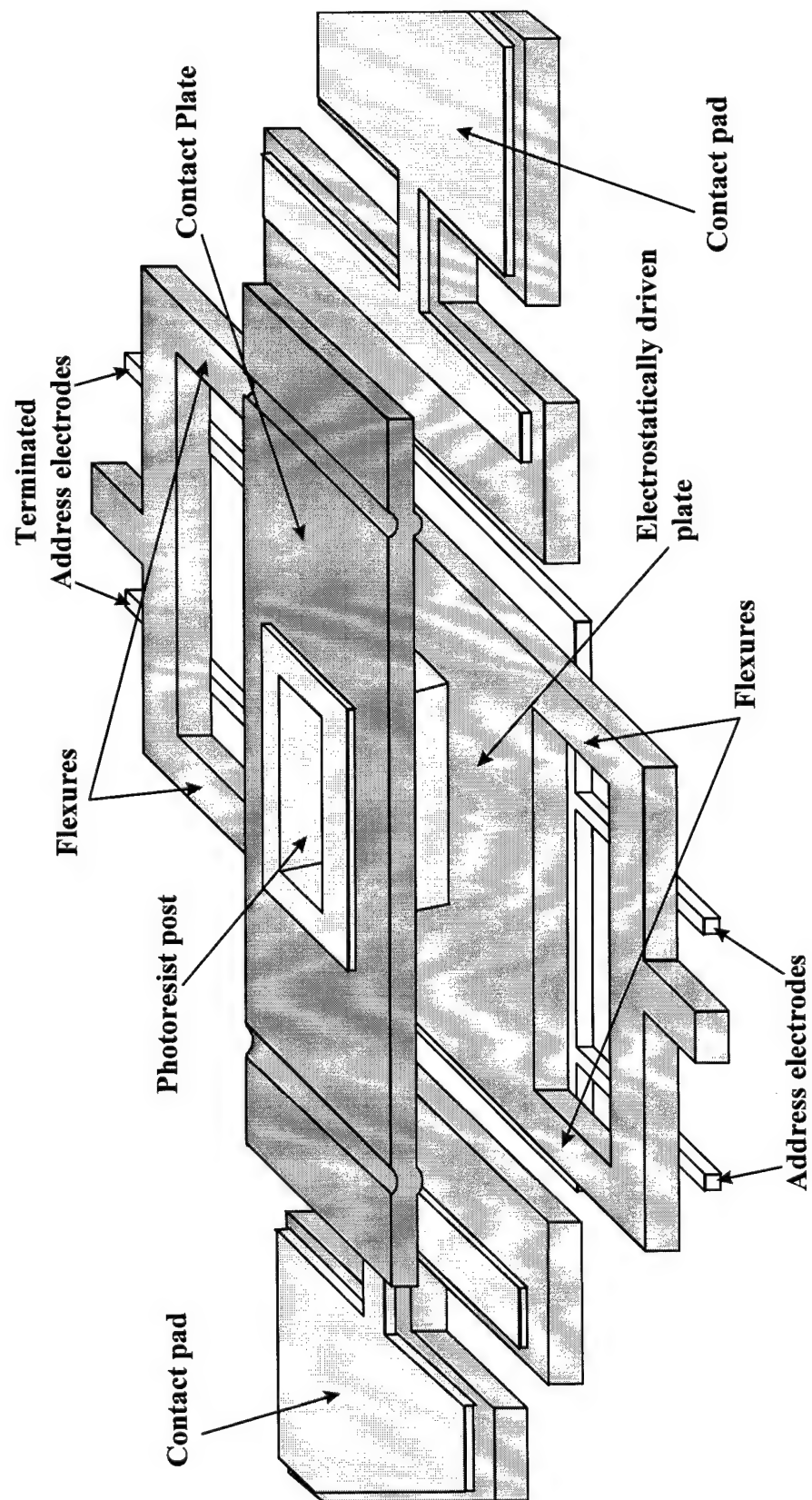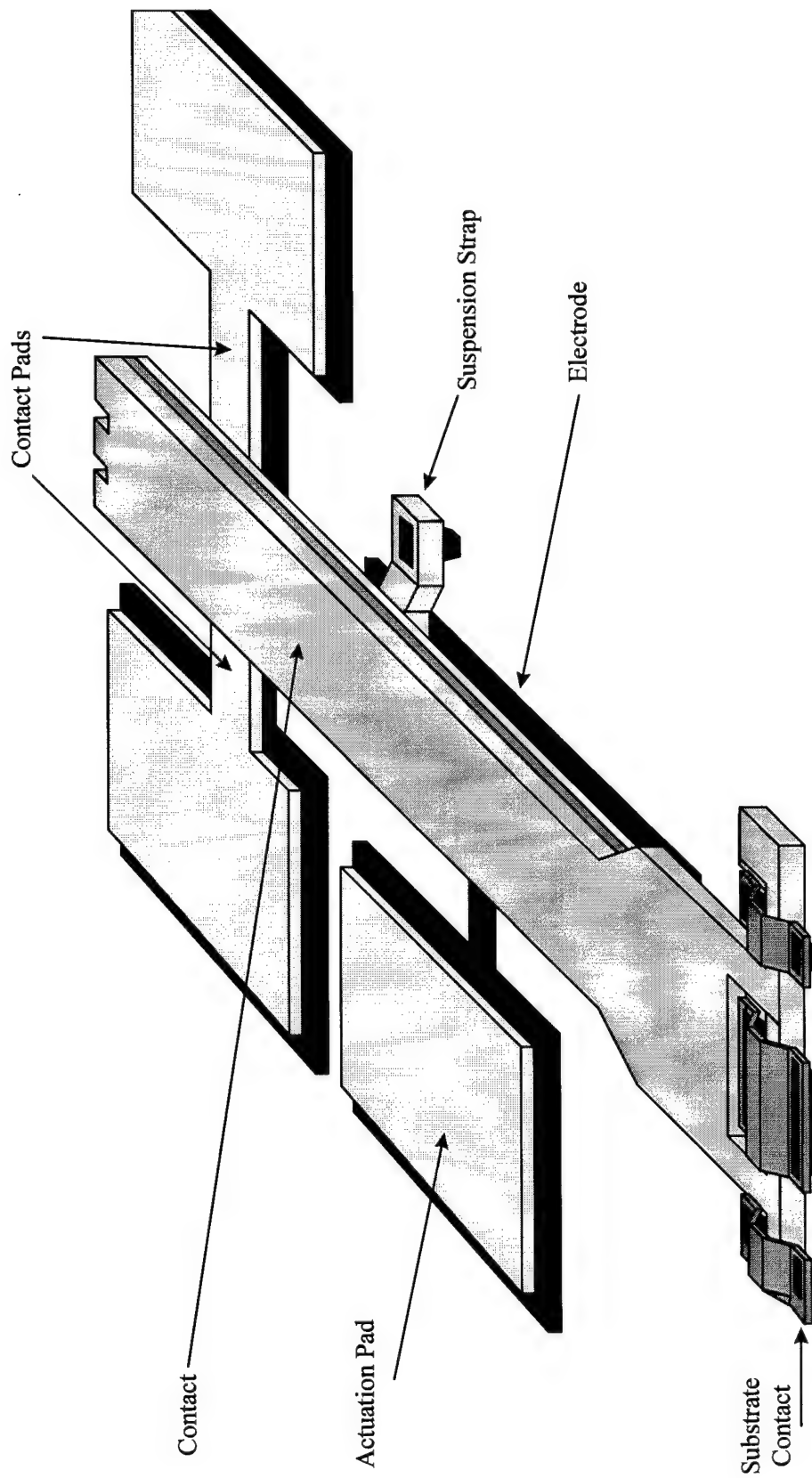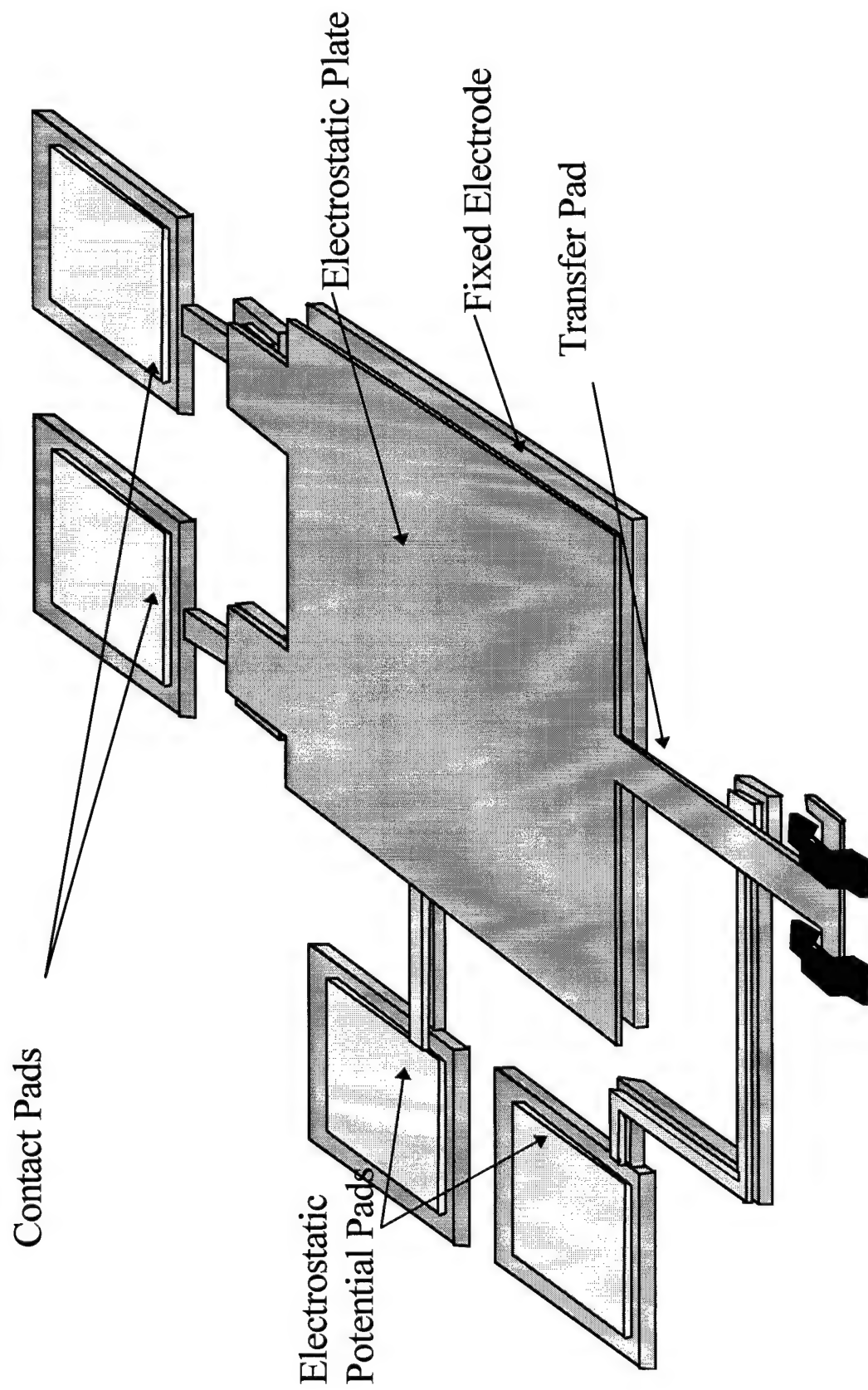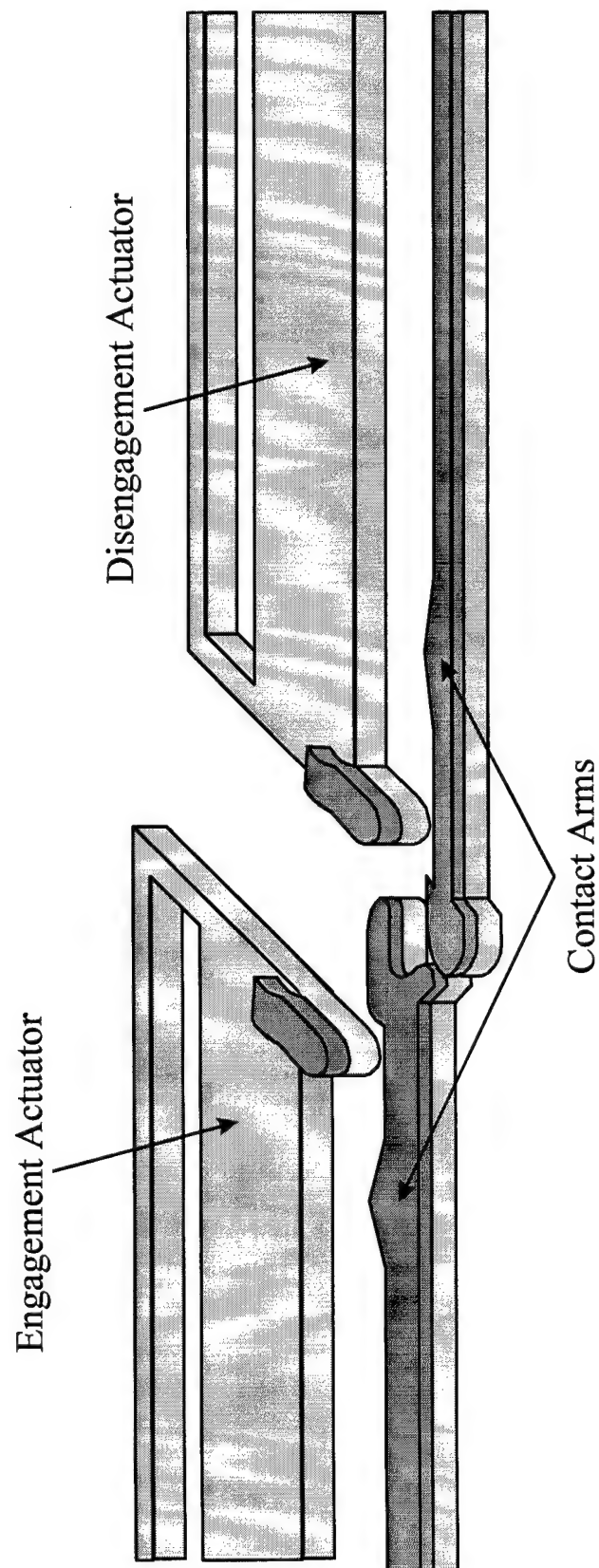
Contact Pads

Direction Making Contact

Flip-over wires

Contact Bar

Engagement

Actuation

Direction Breaking Contact

A-1

Actuation

Engagement
Actuators

Rotor

Pall

Contact Bars

Anchor

A-2

Contact Bar

Direction of Actuation

Contact Ramp

Direction of Actuation

A-3

Gripper Arm

Gripper Arm

Direction of Actuation

Direction of Actuation

Contact Areas

Contact Arm

Direction of Actuation

A-4

Terminated
Address electrodes

Contact Plate

Flexures

Photoresist post

Electrostatically driven plate

Flexures

Contact pad

Address electrodes

Contact pad

A-5

Contact Pads

Suspension Strap

Electrode

Contact

Actuation Pad

Substrate
Contact

A-6

Contact Pads

Electrostatic Plate

Fixed Electrode

Transfer Pad

Electrostatic
Potential Pads

A-7

Disengagement Actuator

Engagement Actuator

Contact Arms

A-8

Electrostatic Plate

Movable Plate

Contact Plate

A-9

Linear Motor

Ratchets

Movable Contact

Stationary Contact

A-10

Contact Bar

Engagement

Flip-over Wires

B-1

Rotator

Contact Bars

Missing Pawl

Engagement actuators

B-2

Contact Bar

Contact Ramp

Engagement Actuators

B-3

Gripper Arms

Contact Area Actuators

Contact Areas

B-4

Contact Plate

Electrostatic Plate
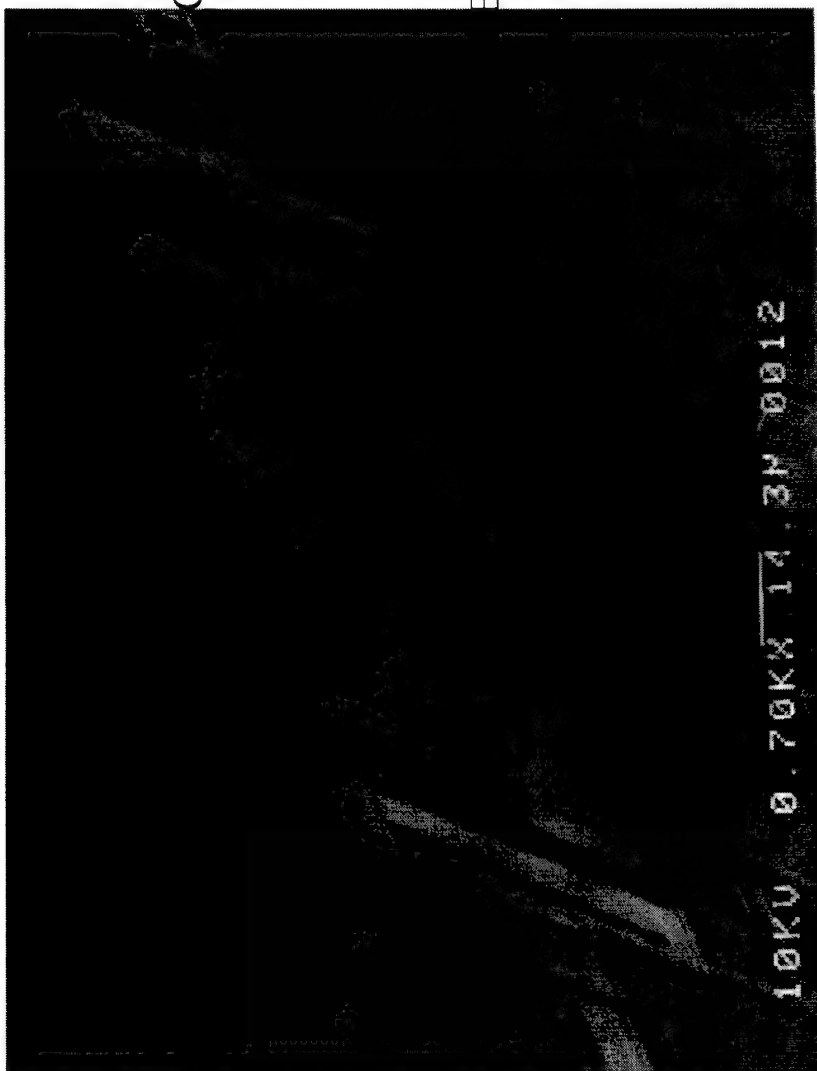
Contacts

Photoresist Post

10KU 0.70KX 14.3M 0012

B-5

pension Strap

trate Contact

rode

Contacts

B-6
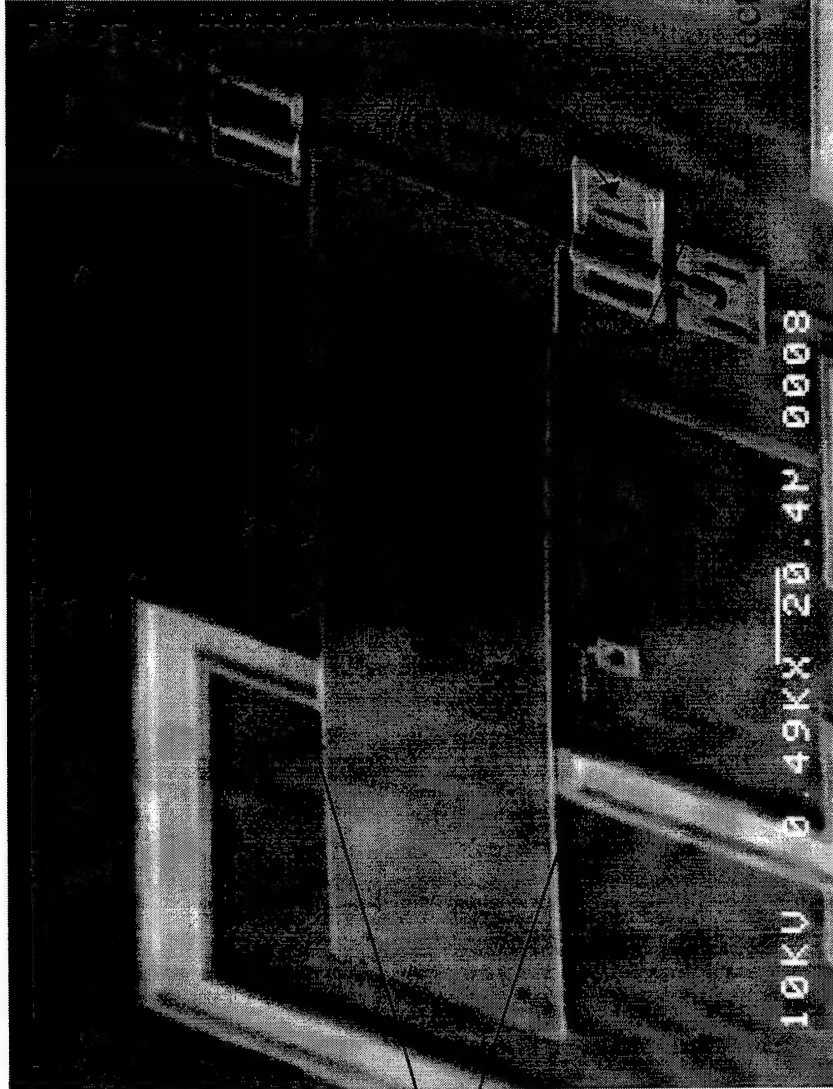
Contact Pads

Electrode

Transfer pad

Contacts

Lock

B-7

Disengagement Actuator

Engagement Actuator

Contact Arms

10KV 1.11KX 9.01μ 0013

B-8

B-9
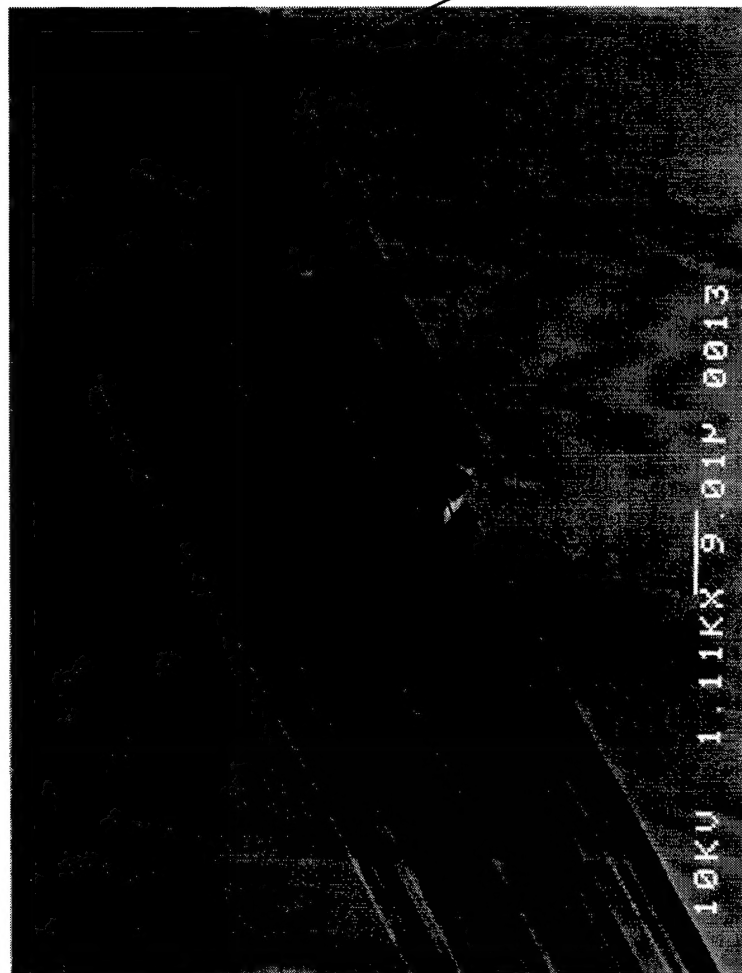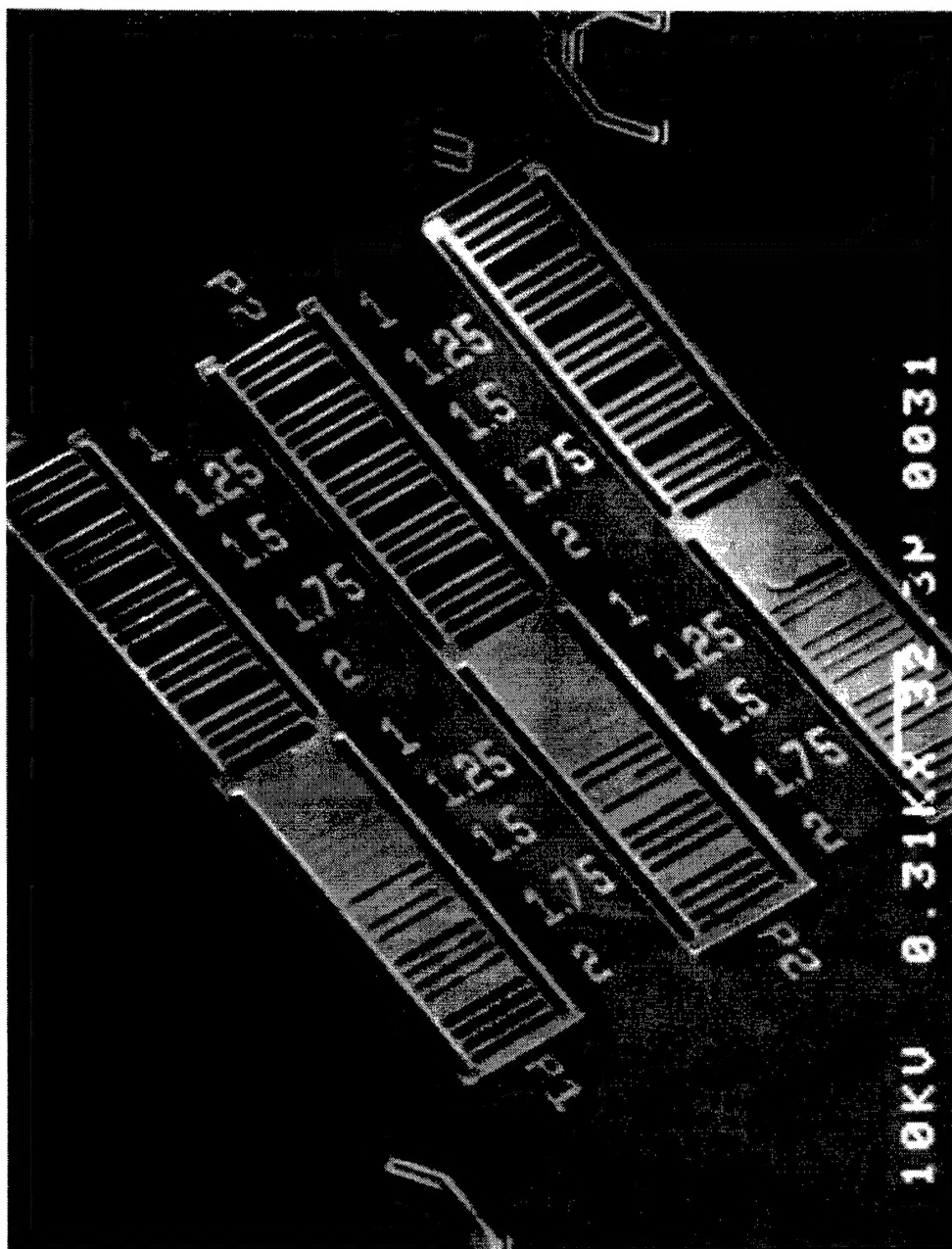
## Vita

Capt Glen A. Kading was born on 17 October 1970 in Omaha, Nebraska. He graduated salutatorian from Bennington High School in 1989 and entered undergraduate studies at the United States Air Force Academy in Colorado Springs, Colorado. In 1993, he graduated with a B.S. in Electrical Engineering and was appointed a second lieutenant in the United States Air Force. Following graduation, he married Doris M. Loos, of Colorado Springs, Colorado on 4 June 1993.

His first assignment was at Wright-Patterson AFB as an acquisition project officer for the EF-111A system improvement program. He moved on to his second assignment while at Wright-Patterson as a test manager in the B-1B system program office. In May 1996, he entered the School of Engineering, Air Force Institute of Technology, and graduated with a Masters of Science in Electrical Engineering, later being assigned to the Air Force Information Warfare Center at Kelly AFB in San Antonio, TX.

Permanent Address: 406 N. 94th St
Omaha, NE 68114

# REPORT DOCUMENTATION PAGE

Public reporting burden for this collection of information is estimated to average 1 hour per response, including the time for reviewing instructions, searching existing data sources, gathering and maintaining the data needed, and completing and reviewing the collection of information. Send comments regarding this burden estimate or any other aspect of this collection of information, including suggestions for reducing this burden, to Washington Headquarters Services, Directorate for Information Operations and Reports, 1215 Jefferson Davis Highway, Suite 1204, Arlington, VA 22202-4302, and to the Office of Management and Budget, Paperwork Reduction Project (0704-0188), Washington, DC 20503.

| 1. AGENCY USE ONLY (Leave blank) | 2. REPORT DATE | 3. REPORT TYPE AND DATES COVERED |
| --- | --- | --- |
| | December 1997 | Master's Thesis |

**4. TITLE AND SUBTITLE**
MICRO-ELECTROMECHANICAL RELAYS FOR MICRO-SATELLITE POWER TRANSFER

**5. FUNDING NUMBERS**

**6. AUTHOR(S)**
Glen A. Kading, Captain, USAF

**7. PERFORMING ORGANIZATION NAME(S) AND ADDRESS(ES)**
Air Force Institute of Technology
2750 P Street
WPAFB OH 45433-7765

**8. PERFORMING ORGANIZATION REPORT NUMBER**

AFIT/GCS/ENG/97D-11

**9. SPONSORING/MONITORING AGENCY NAME(S) AND ADDRESS(ES)**
AFRL/VSSE
Major John H. Comtois
Kirtland AFB NM

**10. SPONSORING/MONITORING AGENCY REPORT NUMBER**

**11. SUPPLEMENTARY NOTES**

**12a. DISTRIBUTION AVAILABILITY STATEMENT**
Approved for public release; distribution unlimited

**12b. DISTRIBUTION CODE**

**13. ABSTRACT** (Maximum 200 words)

In the past few years, micro-electromechanical systems (MEMS) have emerged as a promising new technology with tremendous application potential. One of the possible implementations of MEMS technology is in the development of micro-satellites. It should be possible to mass-produce micro-satellites at a fraction of the cost of one conventional satellite. In order for satellites to be robust, a method of transferring power to systems must be addressed. As micro-satellites are made with conventional integrated circuit technologies at a very small scale, a means of transferring power on a similar scale will be investigated. This research addresses the issue of the design, fabrication, and testing of a MEMS switch for space-based micro-satellites.

Devices are designed and submitted to the Microelectronics Corporation of North Carolina for fabrication. Several different design approaches are attempted, including those using electrostatic and thermal properties for actuation. Fabricated devices are tested using a microprobe station for power usage, power transfer, and frequency characteristics. Devices produce a wide range of results, the best of which transfer large amounts of power in a wide range of frequencies including DC. Recommendations are made to the sponsor agency including the most appropriate designs for use in micro-satellite applications.

**14. SUBJECT TERMS**
Micro-electromechanical systems, micro-switches, MEMS

**15. NUMBER OF PAGES**
108

**16. PRICE CODE**

| 17. SECURITY CLASSIFICATION OF REPORT | 18. SECURITY CLASSIFICATION OF THIS PAGE | 19. SECURITY CLASSIFICATION OF ABSTRACT | 20. LIMITATION OF ABSTRACT |
| --- | --- | --- | --- |
| Unclassified | Unclassified | Unclassified | UL |